SOIL, 7, 453–475, 2021
https://doi.org/10.5194/soil-7-453-2021

SOIL Open Access EGU

The role of geochemistry in organic carbon stabilization against microbial decomposition in tropical rainforest soils

Mario Reichenbach[1], Peter Fiener[1], Gina Garland[2], Marco Griepentrog[2], Johan Six[2], and Sebastian Doetterl[1,2]

[1]Institute of Geography, Augsburg University, 86159 Augsburg, Germany
[2]Department of Environmental System Science, ETH Zurich, 8092 Zurich, Switzerland

Correspondence: S. Doetterl (sdoetterl@usys.ethz.ch)

Received: 17 December 2020 – Discussion started: 5 January 2021
Revised: 17 June 2021 – Accepted: 22 June 2021 – Published: 2 August 2021

Abstract. Stabilization of soil organic carbon (SOC) against microbial decomposition depends on several soil properties, including the soil weathering stage and the mineralogy of parent material. As such, tropical SOC stabilization mechanisms likely differ from those in temperate soils due to contrasting soil development. To better understand these mechanisms, we investigated SOC dynamics at three soil depths under pristine tropical African mountain forest along a geochemical gradient from mafic to felsic and a topographic gradient covering plateau, slope and valley positions. To do so, we conducted a series of soil C fractionation experiments in combination with an analysis of the geochemical composition of soil and a sequential extraction of pedogenic oxides. Relationships between our target and predicting variables were investigated using a combination of regression analyses and dimension reduction. Here, we show that reactive secondary mineral phases drive SOC properties and stabilization mechanisms together with, and sometimes more strongly than, other mechanisms such as aggregation or C stabilization by clay content. Key mineral stabilization mechanisms for SOC were strongly related to soil geochemistry, differing across the study regions. These findings were independent of topography in the absence of detectable erosion processes. Instead, fluvial dynamics and changes in soil moisture conditions had a secondary control on SOC dynamics in valley positions, leading to higher SOC stocks there than at the non-valley positions. At several sites, we also detected fossil organic carbon (FOC), which is characterized by high C/N ratios and depletion of N. FOC constitutes up to 52.0 ± 13.2 % of total SOC stock in the C-depleted subsoil. Interestingly, total SOC stocks for these soils did not exceed those of sites without FOC. Additionally, FOC decreased strongly towards more shallow soil depths, indicating decomposability of FOC by microbial communities under more fertile conditions. Regression models, considering depth intervals of 0–10, 30–40 and 60–70 cm, showed that variables affiliated with soil weathering, parent material geochemistry and soil fertility, together with soil depth, explained up to 75 % of the variability of SOC stocks and $\Delta^{14}C$. Furthermore, the same variables explain 44 % of the variability in the relative abundance of C associated with microaggregates vs. free-silt- and-clay-associated C fractions. However, geochemical variables gained or retained importance for explaining SOC target variables when controlling for soil depth. We conclude that despite long-lasting weathering, geochemical properties of soil parent material leave a footprint in tropical soils that affects SOC stocks and mineral-related C stabilization mechanisms. While identified stabilization mechanisms and controls are similar to less weathered soils in other climate zones, their relative importance is markedly different in the tropical soils investigated.

Published by Copernicus Publications on behalf of the European Geosciences Union.

1 Introduction

1.1 SOC research in the tropics

The tropics are considered potential tipping points for the climate–carbon (C) feedback due to their substantial C storage in the biosphere, fast C turnover and the associated potential C losses to the atmosphere. Despite this key relevance in the terrestrial C cycle and climate regulation, the tropics remain highly underrepresented in research (Schimel et al., 2015). This is especially true for tropical soils, which are estimated to contain approximately one-third of global soil organic carbon (SOC) (Köchy et al., 2015). Many interacting soil processes, both in temperate and tropical soils, are not adequately represented in C turnover models, such as the effect of soil aggregation on soil biota and SOC dynamics (van Keulen, 2001; Wood et al., 2012; Vereecken et al., 2016). Studies analyzing the effect of soil geochemistry on SOC dynamics and stabilization against microbial decomposition combined are also rare (Wattel-Koekkoek et al., 2003; Denef and Six, 2005; Zotarelli et al., 2005; Quesada et al., 2020), and such effects are not included in large-scale C cycle modeling approaches (Vereecken et al., 2016). Most of these geochemical effect studies focus on midlatitudes in the Northern Hemisphere, while the specific conditions under tropical conditions with highly weathered soils remain relatively unknown (Schimel et al., 2015) and can differ greatly compared to temperate soils (Denef and Six, 2006; Denef et al., 2007). Thus, findings from midlatitudes are not easily transferable to tropical soils, since the potential in stabilizing SOC depends on geochemical soil properties that differ fundamentally between geo-climatic zones as a function of pedogenesis. The lack of mechanistic understanding regarding SOC dynamics and their controlling factors creates substantial uncertainties when predicting the future of SOC stocks in the tropics (Schmidt et al., 2011; Shi et al., 2020).

1.2 Environmental and geochemical controls on SOC dynamics in tropical forests

SOC dynamics in tropical rainforests are characterized by high C input and fast C turnover rates (Pan et al., 2011; Wang et al., 2018). Carbon input to soils is mainly driven by root growth and litter production (Raich et al., 2006), both of which are often driven by climatic and hydrological variables that govern vegetation dynamics. Climatic factors such as temperature and precipitation are strong drivers of soil environmental conditions, which can greatly influence soil microbial activity and hence C mineralization and turnover (Davidson and Janssens, 2006; Zhang et al., 2011; Feng et al., 2017). For example, decomposition rates increase in general with temperature, but soil microbial communities adapted to high temperatures are less sensitive to warming (Blagodatskaya et al., 2016). However, climate-driven factors can also influence SOC dynamics indirectly through the interaction with soil factors (Doetterl et al., 2015b). For example, C-depleted tropical subsoils contain small but metabolically active microbial communities contributing to C cycling (Kidinda et al., 2020; Stone et al., 2014). Low soil pH in combination with high clay content dominated by pedogenic oxides can stabilize enzymes on mineral surfaces, which will affect microbial C acquisition (Dove et al., 2020; Allison and Vitousek, 2005; Liu et al., 2020). The accessibility of C for mineralization is predominantly driven by several interacting mechanisms that can stabilize C in soils against microbial decomposition on a decadal up to a millennial timescale (Trumbore 2000; Trumbore, 2009). For example, certain C compounds such as pyrogenic or aromatic C show biochemical resistance since the decomposition of its complex molecular structure is an energy-demanding process and microbes will preferentially consume more easily available organic C forms (Czimczik and Masiello, 2007; Knicker, 2011). Another C fraction that is characterized by long turnover times is fossil organic carbon (FOC), deposited during the formation of sedimentary rocks and often hard to decompose (van der Voort et al., 2019; Kalks et al., 2020). Carbon can also be protected physically against decomposition by encapsulation within soil aggregates. Minerals can also increase the energetic barrier for microorganisms to overcome by forming organo–mineral associations (Oades, 1984; Oades, 1988; von Lutzow et al., 2007; Lehmann et al., 2007; Cotrufo et al., 2013). In particular, it has been shown that the availability of reactive mineral surfaces influences the formation of organo–mineral associations as well (Eusterhues et al., 2003; Jagadamma et al., 2014; Angst et al., 2018). Furthermore, reactive and adsorptive surfaces not only contribute to chemical C stabilization, but also favor the formation of soil aggregates (Simpson et al., 2004; Six et al., 2004; Chenu and Plante, 2006; Lehmann et al., 2007).

While these general types of stabilization against microbial decomposition in the tropics are similar to those in temperate soils, their relative importance and abundance differ greatly due to contrasting weathering history (Six et al., 2002; Denef et al., 2004). Most temperate soils have developed from young (peri)glacial sediments and relatively unweathered bedrock ($\sim$ 15 000 years old). Tropical soils have often been exposed to chemical weathering for millions of years if landforms are stable (Porder et al., 2005; Finke and Hutson, 2008). The resulting soil geochemistry in the tropics is therefore often composed of end-members of weathering products such as secondary minerals (i.e., 1 : 1 low-activity clays, kaolinite) and highly crystalline, pedogenic oxides (West and Dumbleton, 1970). Clay-sized mineral fractions in tropical soils are composed of up to 15 % pedogenic oxides, which is usually much higher than in temperate soils (Ito and Wagai, 2017). While some studies in tropical regions have shown that variation in clay content explains SOC stocks in kaolinitic soils (Quesada et al., 2020), others have shown that SOC stabilization is not affected by clay quantity but instead by the clay mineralogy (Bruun et al., 2010). The most im-

portant identified stabilization mechanisms in kaolinitic tropical soils are mineral–organic associations with short-range-ordered (SRO) pedogenic oxides (Kleber et al., 2005; Bruun et al., 2010; Martinez and Souza, 2020), which stabilize 47 % to 63 % of the bulk SOC stocks in tropical forests (Kramer and Chadwick, 2018). Hence, differences in mineralogy affect a number of key soil fertility parameters and also the way C is stabilized onto minerals, ultimately impacting the interplay between mineral reactivity, microbial community structures and nutrient dynamics (Six et al., 2002; Denef and Six, 2005; Doetterl et al., 2018). For example, SOC stabilization by mineral–organic complexes in tropical soils is highly efficient as they appear in parallel and within highly stable soil aggregates and pseudosand structures (Martinez and Souza, 2020; Quesada et al., 2020). Furthermore, kaolinitic soils can form aggregates rapidly independent from biological processes due to electrostatic interactions between 1 : 1 clay minerals and oxides. But biological processes can lead to stronger organic bonds in soils with 1 : 2 clays, promoting long-term stability (Denef and Six, 2005). This finding relates to the observation that SOC stabilized in kaolinitic 1 : 1 clay soils turns over faster compared to SOC associated with 1 : 2 clay soils (Wattel-Koekkoek et al., 2003). Hence, interactions between geochemistry, aggregation and mineral surface, governed by soil weathering, need to be considered more prominently to understand SOC dynamics in temperate vs. tropical soils.

1.3 Topographic controls on SOC dynamics in tropical forests

In addition to larger-scale biogeochemical and climatic controls of C dynamics, in undulating landscapes soil redistribution processes can highly influence SOC dynamics (van Hemelryck et al., 2010; Doetterl et al., 2016; Wilken et al., 2017). Excessive erosion of topsoils on hillslopes often results in exposure of subsoils with low C contents, which on the one hand can lead to dynamic C replacement (Harden et al., 1999) and on the other hand may stimulate the decomposition of older SOC due to priming with fresh C inputs (Fontaine et al., 2004; Keiluweit et al., 2015). Thereby, removal of weathered topsoils brings new mineral surfaces in contact with fresh C input, which could favor C sequestration due to organo–mineral associations (Doetterl et al., 2016), especially in highly weathered tropical landscapes (Vitousek et al., 2003; Porder et al., 2005). These processes are of potentially great importance for tropical soil systems, as an erosional rejuvenation of land surfaces can bring an entirely different soil mineral composition in touch with the biological C cycle and provide a geochemically entirely different environment for C stabilization against microbial decomposition. Similarly, fossil organic carbon that is brought to the surface might become increasingly decomposed when brought in contact with more active microbial communities compared to subsoil environments. Parallel to these processes of soil denudation, at depositional sites in valleys and at footslopes, former topsoil SOC can become buried by colluvial and alluvial sediments, potentially greatly decreasing microbial decomposition. However, the fate of buried SOC depends greatly on the prevailing environmental conditions in the depositional sites and the sedimentation rates (Gregorich et al., 1998; Berhe et al., 2007; Berhe et al., 2012). Topography can control hydrological patterns in tropical rainforests (Silver et al., 1999; Detto et al., 2013). For example, high water tables lead to lower soil oxygen levels in valley positions, which in turn reduce microbial C decomposition and potentially result in the accumulation of labile SOC. Furthermore, changes in soil water content can cause reductive dissolution of iron oxides, which ultimately affects organo–mineral associations (Berhe et al., 2012). Thus, the interplay between environmental, geochemical and topographic conditions sets the stage for C stabilization and will most likely differ from temperate to tropical soils.

1.4 Study aims

In summary, our current understanding of how geochemistry and topography in highly weathered tropical soils affects SOC stocks and stabilization mechanisms against microbial decomposition is still limited. This study thus aimed to better understand the influence of topography and geochemical properties of soils developed from different parent materials on (i) SOC stocks, (ii) SOC fractions and (iii) SOC stabilization mechanisms in tropical forest soil systems. In addition, (iv) we assessed the contribution of FOC to SOC stocks in sedimentary-rock-derived soils using $\Delta^{14}C$. Within this context, the following hypotheses were tested:

i. SOC stocks and geochemical soil properties sensitive to soil redistribution will vary as a function of a soil's topographic position.

ii. C stabilization mechanisms against microbial decomposition in highly weathered tropical soils, indicated by the amount of C associated with minerals (stable microaggregates and free silt and clay), will be driven by geochemical soil properties as a function of parent material composition.

iii. Fossil organic carbon content in C-bearing parent material will vary as a function of soil depth because it may become accessible for microbial decomposition under surface conditions.

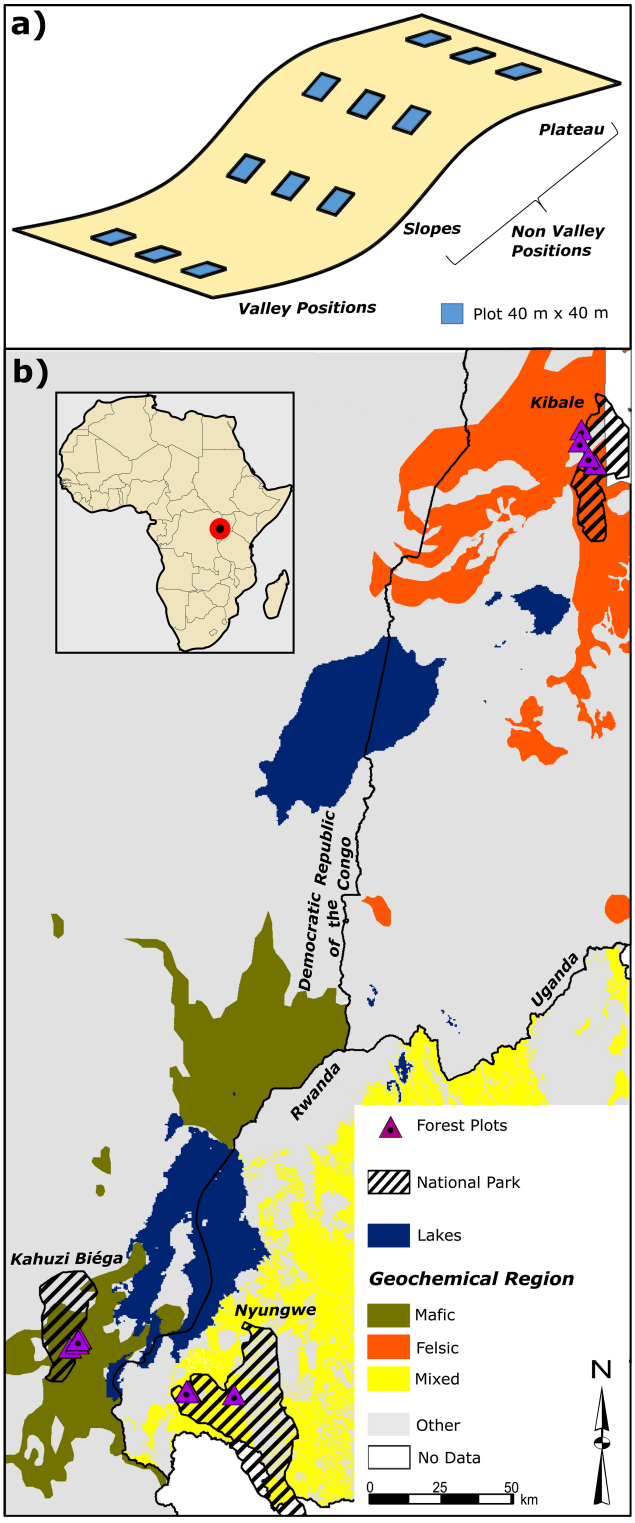

Figure 1. **(a)** Study design used in each geochemical region. **(b)** Overview of study area with respect to soil parent material geochemistry (modified from Doetterl et al., 2021b).

2 Materials and methods

2.1 Study region

The study region is located in the eastern part of the Congo basin and the western part of the Blue Nile basin, with study sites located along the East African Rift Mountain System. Vegetation at all sites is dominated by primary tropical mountain forests (Fig. 1b). Climate of the region is characterized as humid tropical (Köppen Af–Am) with a short dry season (i.e., only 2 months per year with < 50 mm precipitation). The tectonically active rift system resulted in geochemically diverse parent material and in a heterogeneous hilly landscape. The study area consists of parent material ranging from mafic to felsic magmatic bedrock as well as sedimentary rocks of mixed geochemical composition. The undulating landscape resulted in a variety of hydrological conditions at plateau, slope and valley positions. In combination, this makes the study area ideal to analyze the effect of soil geochemistry and topography on SOC stabilization mechanisms against microbial decomposition and stocks in a variety of tropical soils.

Kahuzi-Biega

The study region consisted of three main sites. The Kahuzi-Biega site (from here on called mafic site) is located in the South Kivu province of the Democratic Republic of the Congo (DRC) ($-2.31439°$ S; $28.75246°$ E) with an altitude of 2220 ± 38 m a.s.l. and slopes ranging between 1 %–60 %. The parent material consists of mafic alkali basalts with an age ranging between 9–13 Ma (Schlüter and Trauth, 2006). According to FAO soil classification (FAO, 2014), typical soils in this region are Ferralic Nitisols and Geric Ferralsols. Vegetation is described as a closed broad-leaved semi-deciduous mountain forest (Verhegghen et al., 2012). Mean annual precipitation (MAP) is 1924 mm yr^{-1}, and the mean annual temperature (MAT) is 15.3 °C (Fick and Hijmans, 2017).

Nyungwe

The Nyungwe site (from here on called mixed sedimentary site) is situated in the southwestern part of Rwanda ($-2.463088°$ S; $29.103834°$ E) at 1909 ± 22 m a.s.l. and with slopes ranging between 1 %–60 %. The parent material consists of mixed sedimentary rocks showing alternating layers of quartz-rich sandstone, siltstone and dark clay schists with an age between 1000–1600 Ma (Schlüter and Trauth, 2006). A specific feature of the sedimentary site is the presence of FOC in the parent material of soils ranging between 1.29 %–4.03 % C. FOC in these sediments is further characterized by a high C/N ratio (153.9 ± 68.5), depleted in N and free of ^{14}C (due to the high age of sedimentary rock formation). Typical soils are Geric Ferralsols and Fluvic Gleysols. Vegetation is classified as an afromontane rainforest (van Breugel

et al., 2020). MAP is 1702 mm yr^{-1}, and MAT is 16.7 °C (Fick and Hijmans, 2017).

Kibale

The Kibale site (further called felsic site) is located in western Uganda (0.46225° N; 30.37403° E) with an altitude of 1324 ± 60 m a.s.l. and slopes between 3 %–55 %. The parent material consists of felsic gneissic granites with an age between 1600–2500 Ma (Schlüter and Trauth, 2006). Dominant soils are Geric Ferralsols. Vegetation is classified as Lake Victoria drier peripheral semi-evergreen Guineo–Congolian rainforest (van Breugel et al., 2020). The MAP is 1697 mm yr^{-1} and the MAT is 19.2 °C (Fick and Hijmans, 2017).

2.2 Study design and soil sampling

In the framework of the project TropSOC (Doetterl et al., 2021a, b), soil sampling took place from March to June 2018, applying a stratified random sampling design with triplicate plots of 40 m × 40 m across three topographic positions (i.e., plateau, slope and valley; Fig. 1a) in each geochemical region. Note that because hillslopes were much larger landscape features, we sampled at both topslope and midslope positions. Slope steepness was measured at the center of each plot using a clinometer. Slope length at each plot was derived from a shuttle radar topography mission digital elevation model (SRTM-DEM) (NASA JPL, 2013) with a 30 m × 30 m resolution using the flow direction and flow length tool in ArcMap 10.6.1 (ESRI, USA). Slope length in Kahuzi-Biéga was 70 ± 56 m (max. 170 m), in Nyungwe 101 ± 103 m (max. 339 m) and in Kibale 149 ± 125 m (max. 374 m). No evidence of soil erosion could be observed during the field survey within the plots, and all soil samples were free of carbonates and inorganic C. Attention was paid to install the study plots in areas that are affected by landslides as little as possible. Note that the occurrence of natural landslides cannot be excluded with certainty. However, the vegetation patterns were fairly regular across landforms and replicates. Thus, landslide events can be excluded for the time needed to establish the current vegetation coverages. Additionally, landforms and sampled soils did not show signs of larger erosional events in the recent past. All soils were deeply weathered and showed no signs that would indicate a disturbance event in the past outside of valleys and fluvial systems. Soils were described for every topographic position per geochemical region following WRB classification (FAO, 2014). To describe the chemical composition of the parent material, unweathered bedrock samples were collected in each study area from soil pits, quarries or roadcuts near the plots (maximum distance 15 km). Rock samples from the plots were compared to rock samples from the roadcuts and quarries where possible to ensure that the samples were taken from the same geology.

Each plot was subdivided into four 20 m × 20 m subplots, in which soil profiles were sampled in 10 cm increments down to 1 m soil depth and combined to get depth-explicit composite samples. We then selected three soil layers for further analyses as they represent distinct sections in a soil profile that differ in C input and biogeochemical soil factors: 0–10 cm (topsoil, TS), 30–40 cm (shallow subsoil, SS) and 60–70 cm (deep subsoil, DS). Field-moist samples were sieved to 12 mm to get a homogenous substrate still containing the inherent aggregate structure. Samples were then air-dried for 3–5 d. Soil bulk density samples were taken using Kopecky cylinders. Litter (L) and decomposed organic (O) layers on top of the mineral soil were sampled within a 20 cm × 20 cm square in the center of each subplot and combined to composite samples for the L and O layers, respectively. In total, 36 composite soil cores were sampled on which the soil analysis was conducted (4 cores per plot, combined to one composite, resulting in 12 soil cores per geochemical region distributed across 4 topographic positions in triplicate). In addition, one soil pit of variable depth but always deeper than 100 cm dug in the center in one of three replicate plots per topographic position in each region was described according to FAO guidelines (FAO, 2006). The soils were classified according to the World Reference Base (WRB) soil classification (FAO, 2006). Soils in the mafic region can be described as Umbric, Vetic and Geric Ferralsols and Ferralic Vetic Nitisols. Soils in the felsic regions are classified as Geric and Vetic Ferralols. The mixed sedimentary region shows Geric and Vetic Ferralsols along plateaus and slopes, whereas soils at the valley bottoms are described as Fluvic Gleysols.

2.3 Soil analysis

A wide range of soil physical and chemical parameters were analyzed in the framework of project TropSOC (Doetterl et al. 2021a, b), from which the following were used in this study as potential covariates for controls on SOC: bulk density, total elements of base cations (Ca, Mg, K, Na), total phosphorus, metal oxides with relevance to C stabilization against microbial decomposition (Al, Fe, Mn), elements where concentrations relate strongly to weathering (Si, Ti, Zr) and additional soil properties that relate to soil fertility (texture, pH, effective and potential cation exchange capacity, base saturation, bioavailable phosphorus). Generally, each analysis was performed with 20 % of the samples analyzed in triplicate to assess analytical error. Prior to analyses, all samples were oven-dried at 30 °C for 48–72 h until dry.

Soil C fractionation and nutrient analysis

Three soil size fractions representing different stabilization mechanisms against microbial decomposition associated with varying SOC turnover times were isolated using a microaggregate isolator (Six et al. 2000a; Stewart et al., 2008; Doetterl et al., 2015b). These fractions consisted of

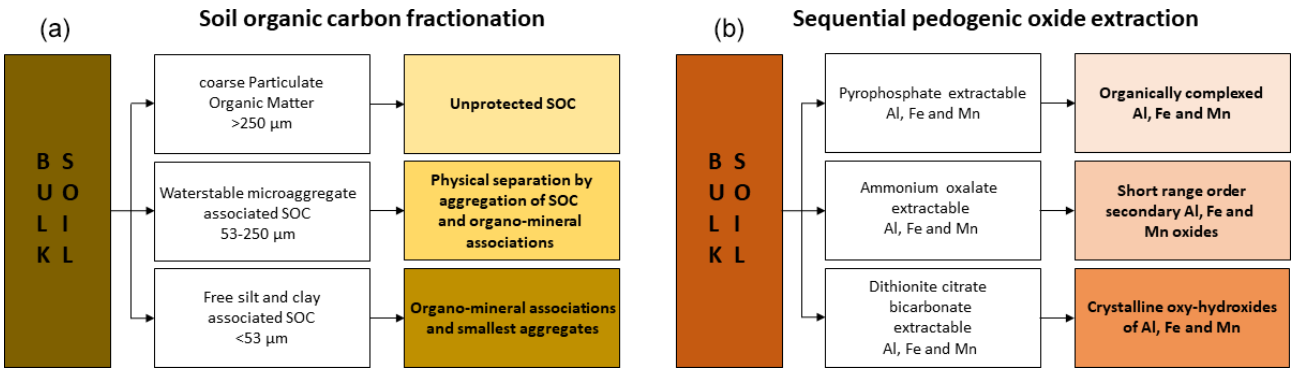

Figure 2. **(a)** Applied SOC fractionation scheme according to Stewart et al. (2008) and Doetterl et al. (2015b) and its interpretation in terms of functional SOC pools and C stabilization mechanisms against microbial decomposition. **(b)** Applied sequential extraction scheme following Stucki et al. (1988) and its interpretation in terms of oxide phases relevant for C stabilization.

(i) $>250\,\mu m$, i.e., unprotected C; (ii) 53–250 µm, i.e., occluded C in microaggregates; and (iii) $<53\,\mu m$, i.e., C associated with free-silt- and-clay-sized particles (Fig. 2). Briefly, 20 g of 12 mm sieved bulk soil was submerged under water for 24 h to break up non-water stable aggregates. Next, the slaked soil sample was wet-sieved through a 250 µm sieve using the microaggregate isolator mounted on a sample shaker. The sample was shaken for 20 ± 11 min with 50 glass beads to break up any remaining macroaggregates. The remaining material was then wet-sieved through a 53 µm sieve by moving the sieve 50 times up and down within 2 min by hand. The isolated soil fractions were then analyzed for carbon and nitrogen (SOC and total nitrogen, TN). To ensure sample homogeneity, the $>250\,\mu m$ fraction was powdered with a ball mill (Mixer Mill MM 200, Retsch, Germany) prior to C and N analysis. The carbon mass of each soil C fraction ($SOC_{>250\,\mu m}$, $SOC_{53-250\,\mu m}$ and $SOC_{<53\,\mu m}$) was calculated by multiplying the SOC concentration by the corresponding fraction mass. The ratio of the C mass of microaggregate-associated C to free-silt- and-clay-associated C (m/s + c ratio) was calculated as a proxy to distinguish between soils in which mineral–C protection, which takes place in both fractions, is amplified by the physical protection through aggregation. It is generally interpreted that the higher this ratio, the more C is occluded within stable microaggregates, on top of being stabilized by mineral–organic interactions (and vice versa for low rations). SOC and TN for all samples were analyzed using dry combustion (Vario EL Cube CNS Elementar Analyzer, Germany). Since the content of rock fragments of all samples was negligible, the SOC stock of the bulk soil (SOC_{bulk}) was calculated by multiplying the SOC concentration by the bulk density and the thickness of the depth increment (10 cm).

Sequential pedogenic oxide extraction

To assess the abundance of Al-, Fe- and Mn-bearing phases and their correlation with SOC_{bulk}, a three-step sequential extraction of pedogenic oxyhydroxides (Stucki et al., 1988) was performed on powdered bulk soil (Fig. 2). First, sodium pyrophosphate at pH 10 was used for extracting organically complexed metals (Bascomb, 1968). Second, ammonium oxalate–oxalic acid at pH 3 was used for extracting amorphous, short-range-order (SRO) secondary oxides and poorly crystalline alumnosilicates (Dahlgren, 1994). Note that results of pyrophosphate extraction must be interpreted with caution, since Al from Al hydroxide phases and poorly crystalline alumnosilicates can also be partially extracted using this reagent (Schuppli et al., 1983; Kaiser and Zech, 1996). Third, dithionite–citrate–bicarbonate (DCB) at pH 8 was used for extracting crystalline oxyhydroxides (Mehra and Jackson, 1958). All extracts including the calibration standards were filtered through 41 grade Whatman filters, diluted (1 : 1000) and then analyzed for elemental concentrations using inductively coupled plasma optical emission spectroscopy (ICP-OES) (5100 ICP-OES Agilent Technologies, USA).

Calculation of FOC contribution to total SOC_{bulk}

The radioisotopic signature ($\Delta^{14}C$) of bulk soil was assessed using AMS (accelerator mass spectrometry) at the Max Planck Institute for Biogeochemistry (Jena, Germany) and conventional radiocarbon age following the conventions of Stuiver and Polach (1977). ^{14}C radiocarbon dating was used to estimate the relative age differences of C between samples and to estimate the potential contribution of FOC to the total SOC in soils developed from mixed sedimentary rocks. Following Cerri et al. (1985) and Kalks et al. (2020), we assume that the biogenic carbon in the different soil depths of all sites was relatively similar and overall several orders of magnitude younger than the FOC. The baseline

values for this assumption are the depth-explicit mean values of $\Delta^{14}C$ of the mafic and felsic sites as they are free of FOC. Based on this assumption, the mean depth-specific percent modern carbon (PMC) values for those regions were calculated as follows:

$$f_{\text{bio}} = \frac{F}{F_{\text{bio}}} \cdot 100, \quad (1)$$

where F is the PMC in a sample, f_{bio} (%) is the proportion of biogenic organic carbon in the total amount of organic carbon and F_{bio} is the fraction PMC averaged from the plateau and slope sites and depths of the mafic and felsic sites.

In a second step, the amount of FOC at the mixed sedimentary site was assessed as follows:

$$f_{\text{FOC}} = 100 - f_{\text{bio}}, \quad (2)$$

where f_{FOC} is the proportion of fossil organic carbon as a fraction of the total amount of soil organic carbon (%).

Calculation of the chemical index of alteration and elemental differences between parent material and soil

Based on results of the analyses of total element concentrations (see Doetterl et al., 2021b for details), the chemical index of alteration (CIA, in %) (Fiantis et al., 2010) was calculated to assess the weathering stage of the soil as follows:

$$\text{CIA} = \frac{\text{Al}_2\text{O}_3}{\text{Al}_2\text{O}_3 + \text{CaO} + \text{Na}_2\text{O} + \text{K}_2\text{O}} \cdot 100. \quad (3)$$

To illustrate gains and losses of nutrients in the soil column compared to the underlying parent material, the relative and absolute difference in element concentration for key elements that enrich or deplete with weathering (ΔCa, ΔK, ΔMg, ΔNa, ΔP, ΔFe, ΔAl, ΔMn, ΔSi) were assessed using unweathered bedrock samples and soil collected from 30–40 cm depth at the plateau position in each geochemical region. This location and depth was chosen as it (i) represents the most weathered part of the soil column, (ii) excludes any potential influence by lateral fluxes and (iii) reduced the likelihood of biogenic disturbance through root growth, which is concentrated in our sites in organic layers and topsoil (Doetterl et al., 2021b).

2.4 Statistical analysis

The significance level for all statistical analysis was set at $p < 0.05$. Differences with depth, topography and geochemistry of the region for the various SOC fractions and SOC-related variables described above were assessed by testing for equality of means using one-way and Welch analysis of variance (ANOVA) ($n = 3$ for plateaus, $n = 6$ for slopes and $n = 3$ for valleys). To avoid type I errors in ANOVA caused by heteroscedasticity (Moder, 2007), we performed Levene's test (Levene, 1960) for all ANOVA. Based on the outcome of the Levene's test, the result of either one-way ANOVA (no heteroscedasticity) or of the Welch ANOVA (heteroscedasticity present) was used. To compare the means of multiple groups, post hoc pairwise comparison was applied using Bonferroni correction (Day and Quinn, 1989) or Tamhane T2 in the case of unequal variances (Tamhane, 1979).

For dimension reduction of independent potential predictors of SOC, to illustrate the variance of these predictors across the dataset, and to minimize multicollinearity in regression analyses, we performed a varimax-rotated principal component analysis (rPCA) ($n = 27$) using all non-SOC-derived chemical and physical soil variables described above. Only predictor variables with a loading factor of > 0.5 or < -0.5 were interpreted for each rotated component (RC). Because of differences in units and ranges of predictor variables, prior to the rPCA, a Z-score standardization (Lacrose, 2004) was applied as follows:

$$X^* = \frac{X - \text{mean}(X)}{\text{SD}(X)}, \quad (4)$$

where X^* is the standardized value, X is the original value and SD is the standard deviation.

Only RCs with an eigenvalue > 1 and explaining $> 5\,\%$ variances were kept for further statistical analyses. A mechanistic interpretation of the identified RCs was provided based on the loading of each RC.

The remaining RCs were used as explanatory variables in multiple linear stepwise regressions to the most important predictors explaining differences in SOC variables. We focused our analyses on predicting SOC_{bulk} and $\Delta^{14}C$, as well as m/s + c ratios for non-valley positions ($n = 27$). Valley positions were excluded due to the small sample size ($n = 9$). As most of these variables naturally show strong depth trends (Minasny et al., 2016), we added soil depth as an additional explanatory variable in our models to avoid overinterpretation of variables, which were cross-correlated with soil depth. After assessing the predictive model strength of our multi-RC models on SOC target variables, we assessed the relative importance of explanatory variables using the R package Relaimpo (Grömping, 2006). In a final step, to disentangle the effect of soil depth and RCs to predict our SOC target variables, partial correlation was used by controlling correlations of RCs to explore whether SOC variables were directly controlled by the rPCs after controlling for soil depth. IBM SPSS Statistics 26 (IBM: SPSS Statistics for Windows, 2019) was used for the ANOVA and partial correlation. The rPCA, regressions and relative importance analysis were realized using R 3.6.1 (R Core Team, 2020).

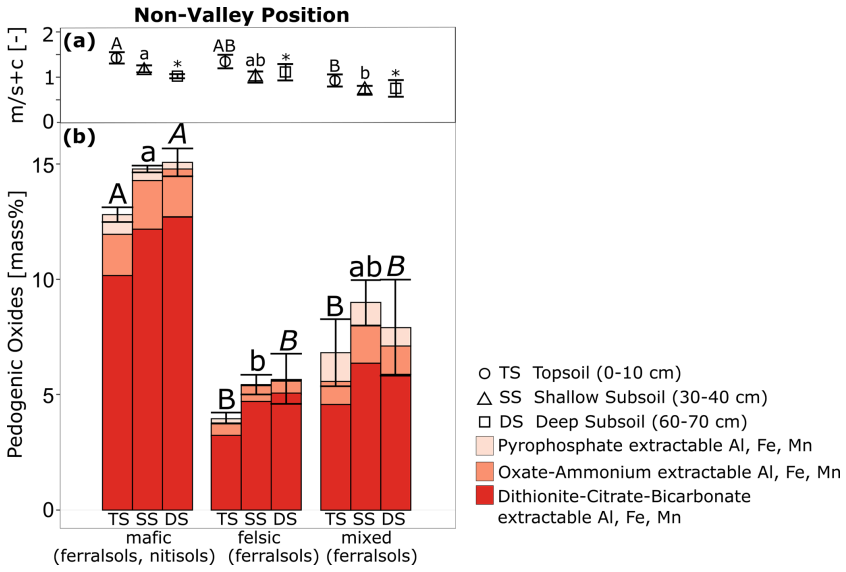

Figure 3. **(a)** m/s + c ratio ($n = 9$ per bar) and **(b)** pedogenic oxide fractions ($n = 3$ per bar) of the sequential extraction across geochemical regions in non-valley positions. Where letters share the same font type, means were compared to each other, with letters indicating significant differences between geochemical regions per soil depth for m/s + c ratio **(a)** and total pedogenic oxide mass **(b)**. Asterisks indicate no significant differences in means ($p > 0.05$). The error bar represents standard error.

3 Results

3.1 Climate and topography

Note that we have pretested for correlations between SOC stocks, mean annual temperature (MAT) and mean annual precipitation (MAP) across our study sites. No significant correlations were found with the included climatic variables (Table A1), indicating no significant effect of climatic variation between sites on SOC dynamics. Hence, we focused our further analyses on the impact of local geochemistry and topography on SOC stocks and stabilization against microbial decomposition.

For all tested SOC variables, significant differences in the means of different topographic positions within each geochemical region were found between valley and non-valley positions (plateaus and slopes) with higher SOC stocks in valley positions compared to non-valley positions. No significant differences were found between plateau and slope positions (Table A2). Even though valley positions are of the same geochemistry as the non-valley positions, geochemical soil properties in valleys were significantly different than at non-valley positions, as fluvial activity and sedimentation unrelated to hillslope processes were dominant (see Supplement 1 for additional results and discussion on valley positions). Consequently, for all follow-up analyses on differences with soil depth and geochemistry, the dataset was split into valley positions vs. non-valley positions. Due to the limited sample size for the valley positions ($n = 1$–3), no further statistical analysis was applied. However, all valley data are available in a short supplementary result and discussion section attached to this paper (Supplement 1).

3.2 Soil chemical weathering stage and pedogenic oxides

Parent material geochemistry and weathering stage

Parent material, from which soils in the three geochemical regions have developed, showed distinct differences in elemental composition (Doetterl et al., 2021a, b), with generally low concentrations of Ca, Mg and Na base cations (0.01–0.58 wt %). Al and Fe concentrations were significantly higher in the mafic (Al: 6.27 ± 2.84; Fe: 8.98 ± 1.84 mass%) than sedimentary rocks region (Al: 0.62 ± 0.41; Fe: 2.32 ± 1.73 mass%) and the felsic region (Al: 0.52 ± 1.21; Fe: 1.09 ± 1.58 mass%). Similarly, total P was highest in the mafic region (P: 0.37 ± 0.14 mass%) compared to the mixed sedimentary (P: 0.02 ± 0.02 mass%) and the felsic region (P: 0.01 ± 0.1 mass%). In contrast, Si content was lowest in the mafic region (Si: 14.22 ± 2.01 mass%) compared to the mixed sedimentary rocks region (Si: 36.11 ± 7.01 mass %) and the felsic region (Si: 37.29 ± 5.92 mass%).

Across geochemical regions, soils were highly weathered, as indicated by high CIA values of 78 %–99 % at all three soil depths (data not shown). Soils developed from mafic parent material were depleted in Ca, Mg and Na base cations compared to parent material (Ca: −38 % to −100 %; Mg: −72 % to −87 %; Na: −90 % to 375 %). Soils developed in the mixed sedimentary region were depleted in Ca

(-100 ± 172 %) compared to parent material but not for Mg or Na. Soils developed from felsic parent material showed a substantial increase in all base elements (Ca: up to 1240 %; Mg: up to 1015 %; Na: up to 677 %). All soils were enriched in Al compared to parent material (mafic: up to 307 %; felsic: up to 6859 %; mixed sedimentary: up to 1514 %). Similarly, all soils were enriched in Fe compared to parent material (mafic: up to 85 %; felsic: up to 1482 %; mixed sedimentary: up to 3486 %). Soils developed from mafic parent material showed depletion in P (-72 % to 14 %) compared to the parent material. In contrast, we observed an enrichment in P for soils developed from mixed sedimentary (up to +2583 %) and felsic parent material (up to 6671 %) compared to parent material. Note that the extraordinarily high differences in P between soil and parent material in the latter regions are mainly related to the fact that P concentrations in parent material of the felsic and sediment region were extremely small to begin with but did accumulate in soil through fixation in the biosphere and plant uptake (Wilcke et al., 2002; Wang et. al., 2010). This interpretation is supported by the observations that P mass in all three geochemical regions for the investigated soil layers used for comparison to parent material converges (mafic: 0.15 ± 0.002 mass%; felsic: $0.05 \pm$ N/A mass%; mixed sedimentary: 0.08 ± 0.01 mass%), while other less critical elements for biological processes leached during soil development. For example, all soils were depleted in Si compared to the parent material (mafic: -27 % to 8 %; felsic: -62 % to -26 %; mixed sedimentary: -71 % to -58 %), which is indicative of long-term weathering.

Pedogenic oxides

For non-valley positions, pyrophosphate-extractable oxides (0.02 to 1.93 mass%) and oxalate-extractable oxides (0.32 to 2.33 mass%) were low compared to DCB-extractable oxides (2.74 to 13.63 mass%) (Fig. 3). Pyrophosphate-extractable oxides showed no significant differences across geochemical regions. Oxalate-extractable oxides were significantly higher across all soil depths in mafic (1.68 to 2.33 mass%) and mixed sedimentary (0.32 to 2.28 mass%) soils compared to soils developed from felsic parent material (0.35 to 0.91 mass%). DCB-extractable oxides across all soil depths were significantly higher in mafic soils (9.54 to 13.63 mass%) compared to soils developed from felsic (2.74 to 7.03 mass%) and mixed sedimentary parent material (3.55 to 8.44 mass%).

3.3 Variation in SOC properties with geochemistry

SOC_{bulk}

SOC_{bulk} in topsoil did not differ across geochemical regions (mafic: $50.6 \pm 13.9\,t\,C\,ha^{-1}$; felsic: $45.3 \pm 3.9\,t\,C\,ha^{-1}$; mixed sedimentary: $44.0 \pm 3.9\,t\,C\,ha^{-1}$), whereas subsoil SOC_{bulk} was significantly smaller in the felsic region (shallow subsoil: $16.3 \pm 2.5\,t\,C\,ha^{-1}$; deep subsoil: $10.1 \pm 1.9\,t\,C\,ha^{-1}$) compared to the mafic (shallow subsoil: $28.3 \pm 3.3\,t\,C\,ha^{-1}$; deep subsoil: $22.9 \pm 7.2\,t\,C\,ha^{-1}$) and mixed sedimentary region (shallow subsoil: $30.4 \pm 2.8\,t\,C\,ha^{-1}$; deep subsoil: $23.9 \pm 4.7\,t\,C\,ha^{-1}$). Note that while SOC_{bulk} decreased strongly with depth in the mafic and felsic region, only a weak decrease in SOC_{bulk} with depth was observed in the mixed sedimentary region (Fig. 4).

Table 1. Proportion of biogenic- vs. fossil-derived organic carbon (OC) in soils developed from mixed sedimentary rocks in non-valley positions ($n = 3$). FOC values in felsic and mafic soils were 0 % (data not shown).

Depth increment	Amount of biogenic OC (%)	Amount of fossil OC (%)
0–10 cm	88.7 ± 2.6	11.3 ± 2.6
30–40 cm	60.7 ± 14.5	39.3 ± 14.5
60–70 cm	48.0 ± 13.2	52.0 ± 13.2

Abundance of C fractions

At all sites and soil depths, fractions were dominated by microaggregate-associated C ($SOC_{53-250\,\mu m}$), contributing 32.6 ± 9.9 % to 55.2 ± 1.4 % of SOC_{bulk}, and free-silt-and clay-associated C ($SOC_{<53\,\mu m}$), contributing 40.3 ± 4.8 % to 54.5 ± 2.4 % of SOC_{bulk}. Coarse particulate organic carbon ($SOC_{>250\,\mu m}$) contributed 1.4 ± 0.2 % to 11.1 ± 1.5 % of SOC_{bulk}. Microaggregate-associated C and m/s + c ratios were generally higher in topsoils ($SOC_{53-250\,\mu m}$: 43.19 ± 6.77 % to 55.23 ± 1.43 %; m/s + c: 0.93 ± 0.17 to 1.42 ± 0.04) compared to subsoils ($SOC_{53-250\,\mu m}$: 32.64 ± 9.88 % to 49.65 ± 1.84 %; m/s + c: 0.75 ± 0.2 to 1.07 ± 0.35) (Fig. 3a). For topsoil and shallow subsoil, the m/s + c ratio was significantly higher in the mafic region than in the sediment region, meaning more microaggregate-associated C in mafic than in mixed sediments compared to free-s+c-associated C. The felsic region ranges between the other two geochemical regions in this regard and was not significantly different to either one. Deep subsoil m/s + c indicated the same trends but was not statistically different across regions (Fig. 3a). Note that the relative abundance of microaggregate-associated and free silt and clay associated with C was not significantly different with topographic positions (Table A2).

Changes in ^{14}C signature

Soils from all geochemical regions at non-valley positions were significantly more depleted in $\Delta^{14}C$ with increasing soil depth (Fig. 4a and b). The $\Delta^{14}C$ ranged from 31.2 ± 11.5 ‰ (mafic) to -78.7 ± 26.6 ‰ (mixed sedimentary) in the topsoil and -257.8 ± 32.8 ‰ (mafic) to

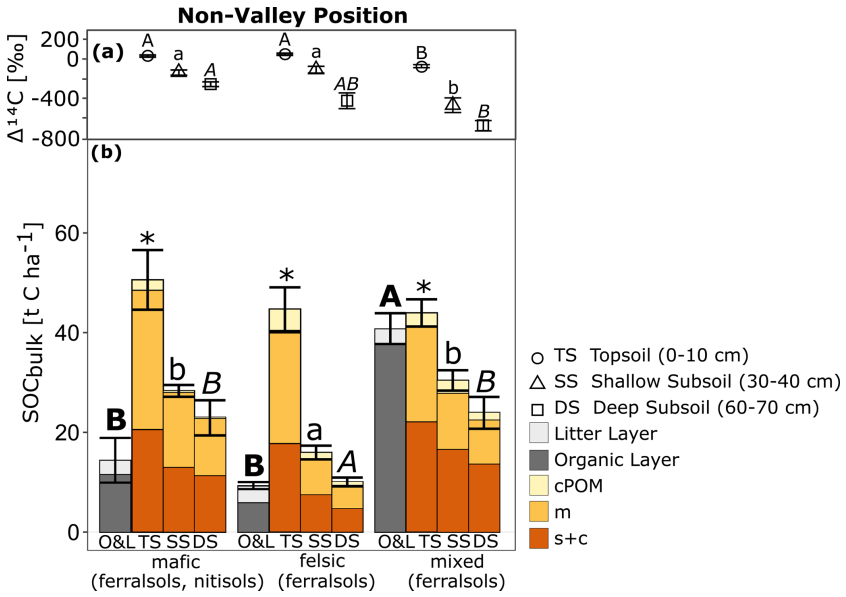

Figure 4. **(a)** $\Delta^{14}C$ across geochemical regions in non-valley positions ($n = 3$ per bar). **(b)** SOC_{bulk} and fractions across geochemical regions in non-valley positions ($n = 9$ per bar). Where letters share the same font type, means were compared to each other, with letters indicating significant differences between geochemical regions per soil layer for $\Delta^{14}C$ **(a)** and SOC_{bulk} **(b)**. Asterisks indicate no significant differences in means ($p > 0.05$). For $\Delta^{14}C$ values, error bars are smaller than symbols. cPOM – coarse particulate organic matter, m – stable microaggregates, s+c – free silt and clay fraction.

-675.2 ± 89.6 ‰ (mixed sedimentary) in subsoil. While there were no significant differences between $\Delta^{14}C$ of comparable samples of the felsic and mafic region, their counterparts from the mixed sedimentary region were significantly more depleted in $\Delta^{14}C$. The contribution of FOC to soil C in the mixed sedimentary region increased significantly with soil depth for non-valley positions, ranging from 11.3 ± 2.6 % FOC in topsoils to 52.0 ± 13.2 % in subsoils (Table 1).

3.4 Rotated principal component explained variance and loadings

Four rPCs were determined (rPC_{nv}) explaining 78.1 % of the variance in the non-valley position subset (Fig. 5; Table A4). $rPC1_{nv}$ (eigenvalue 9.34, explaining 33.4 % of the variance) represents solid-phase mineralogy, in which total metal oxide concentration ($\sum$ Fe, Al, Mn), DCB-extractable oxide concentration and the Al/Si ratio had strong positive loadings (variable loading > 0.9), while Si, the pH/clay ratio and sand content had strong negative loadings (< -0.7). $rPC2_{nv}$ (eigenvalue 9.15, explaining 32.7 % of the variance) represents the chemistry of the soil solution where exchangeable bases, the cation exchange capacity (CEC) base saturation/clay ratio and the Ca/Ti ratio showed strong positive loadings (≥ 0.87), and exchangeable acidity, CIA and $SOC_{organic}$ showed strong negative loadings (< -0.5). $rPC3_{nv}$ (eigenvalue 1.82, explaining 6.5 % of the variance) represents silt content and the C stock of organic layers ($SOC_{organic}$), both having a strong negative loading (< -0.5). $rPC4_{nv}$ (eigenvalue 1.57, explaining 5.6 % of the variance) represents organo–mineral complexes, with pyrophosphate-extractable oxide concentration showing a strong positive loading (< 0.8).

3.5 Explained variability and relative importance of predictors (non-valley soils)

Soil depth and $rPC4_{nv}$ explained 73 % of variability (R^2) in SOC_{bulk} ($p < 0.01$). Soil depth contributed 82 % to the explanatory power of the model (Table 2). The second most important explanatory variable in our model was $rPC4_{nv}$, which represented organo–mineral complexes ($p < 0.01$) and contributed 18 % to the explanatory power of the model. Soil depth and $rPC1_{nv}$, $rPC3_{nv}$ and $rPC4_{nv}$ could explain 75 % of variability (R^2) in $\Delta^{14}C$ data ($p < 0.01$). Soil depth contributed 75 % to the explanatory power of the model, followed by $rPC3_{nv}$ (silt content, 16 % explanatory power), $rPC4_{nv}$ (organo–mineral complexes, 5 % explanatory power) and $rPC1_{nv}$ (solid-phase mineralogy, 4 % explanatory power). Soil depth, $rPC1_{nv}$ and $rPC2_{nv}$ could explain 44 % of variability (R^2) in the m/s+c ratio ($p < 0.01$). $rPC2_{nv}$ contributed 46 % to the explanatory power of the model, followed by $rPC1_{nv}$ (solid-phase mineralogy, 31 % explanatory power) and soil depth (23 % explanatory power), making m/s+c ratios the only SOC target variable not highly correlated with soil depth.

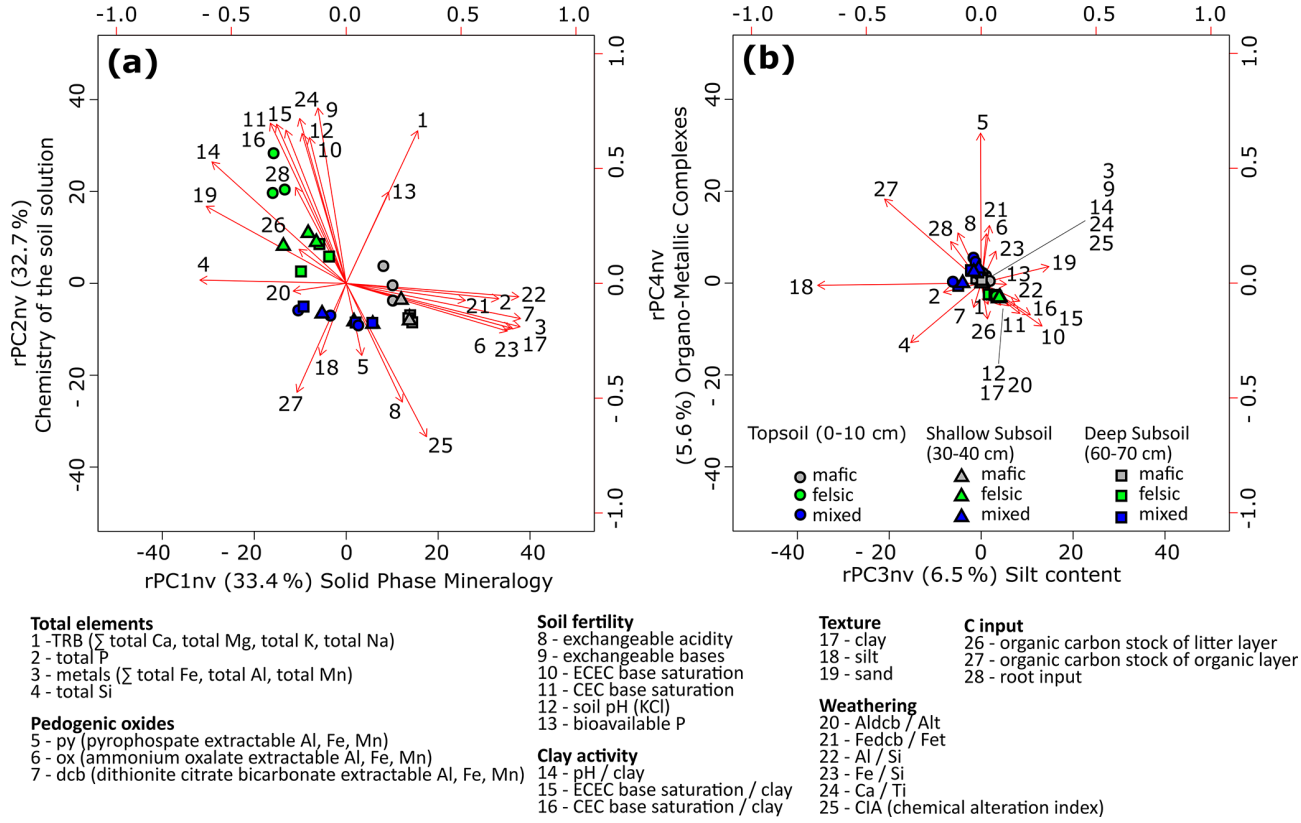

Figure 5. Biplots of the varimax-rotated principal component analysis. **(a)** $rPC1_{nv}$ and $rPC2_{nv}$ and **(b)** $rPC3_{nv}$ and $rPC4_{nv}$ of non-valley positions ($n = 27$). Observations cluster together based on similarities within geochemical regions and their distinction to other geochemical regions. Vector length indicates how strongly variables influence a specific rPC. The angles between vectors display the degree of autocorrelation between variables. Small angles represent positive correlations and high degree of autocorrelation, diverging angles represent negative correlations and a high degree of autocorrelation, and high angles indicate no correlations between variables and/or rPCs.

Table 2. Multiple linear stepwise regression analysis (beta coefficients) and relative importance analysis in brackets for non-valley soils. SOC_{bulk}, $\Delta^{14}C$ and the m/s + c ratio are explained by soil depth and the extracted rPCs. Adjusted R^2 displays the goodness of fit, and the root mean square error (RMSE) assesses the model quality.

Response	Soil depth	$rPC1_{nv}$ – solid-phase mineralogy	$rPC2_{nv}$ – chemistry of the soil solution	$rPC3_{nv}$ – silt content	$rPC4_{nv}$ – organo-mineral complexes	Adjusted R^2	RMSE
SOC_{bulk}	-0.77^{c} (82 %)				0.31^{c} (18 %)	0.73	0.46
$\Delta^{14}C$	-0.87^{c} (75 %)	0.39^{b} (4 %)		0.24^{a} (16 %)	-0.32^{a} (5 %)	0.75	0.47
m/s + c	-0.29^{a} (23 %)	0.74^{c} (31 %)	0.8^{c} (46 %)			0.44	0.39

[a] $p < 0.1$. [b] $p < 0.05$. [c] $p < 0.01$.

Table 3. Partial correlation analysis between SOC variables (SOC_{bulk}, $\Delta^{14}C$ and m/s+c ratio) and extracted rPCs controlling for soil depth. Zero-order correlation displays the Pearson r value when including no control variable. The controlled correlation shows the Pearson r value when controlling for soil depth.

		$rPC1_{nv}$ – solid phase mineralogy		$rPC2_{nv}$ – chemistry of the soil solution		$rPC3_{nv}$ – silt content		$rPC4_{nv}$ – organo-mineral complexes	
Response	Control	Pearson r	R^2	Pearson r	R^2	Pearson r	R^2	Pearson r	R^2
SOC_{bulk}	zero-order	0.06	0.00	0.05	0.00	−0.19	0.04	0.41[b,d]	0.17
	soil depth	0.41[b,d]	0.17	−0.39[b,f]	0.15	−0.41[b,g]	0.17	0.53[c,d]	0.28
$\Delta^{14}C$	zero-order	−0.05	0.00	0.44[b,d]	0.19	0.41[b,d]	0.17	−0.13	0.02
	soil depth	0.19	0.04	0.31[e]	0.10	0.57[c,d]	0.32	−0.35[a,f]	0.12
m/s + c	zero-order	0.13	0.02	0.38[a,e]	0.14	0.46[b,d]	0.21	−0.22	0.05
	soil depth	0.23	0.05	0.29	0.08	0.47[b,d]	0.22	−0.30[f]	0.09

[a] $p < 0.1$. [b] $p < 0.05$. [c] $p < 0.01$. Pearson's r and R^2 values derive from simple linear regression between the individual rPCA and the respective SOC variable. [d] $r > 0.4$. [e] $r > 0.3$. [f] $r < -0.3$. [g] $r < -0.4$.

3.6 Partial correlations controlled for soil depth

When controlling for soil depth, correlations between SOC_{bulk} and the identified rPCs became significant, with changes in correlation coefficients ranging from 0.01 to 0.44 (Table 3). Solid-phase mineralogy explained 16.8 %, chemistry of the soil solution 15.2 %, silt content 16.8 % and organo–mineral complexes 28.1 % of the variability (R^2) in SOC_{bulk}. Correlation between $\Delta^{14}C$ and the chemistry of the soil solution became insignificant and declined by 0.13, whereas the correlation of silt content and organo–mineral complexes improved by 0.16 and 0.22, respectively. Silt content explained 32.5 %, and organo–mineral complexes explained 12.3 % of the variability (R^2) in $\Delta^{14}C$. Correlation between the m/s + c ratio and chemistry of the soil solution decreased by 0.09, with only silt content left with a significant correlation. Silt content explained 22.1 % of the variability (R^2) in the m/s + c ratio.

4 Discussion

4.1 Soil C stabilization against microbial decomposition driven by soil chemistry and parent material

In contrast to our initial hypothesis that topography affects C stabilization in tropical forest soils through lateral material movements, we found no indication of this in our analysis (see the Supplement and short discussion therein). Despite prolonged chemical weathering, parent material leaves an identifiable, long-lasting footprint in the chemical properties of tropical forest soils (Fig. 5). Overall, the differences in elemental composition between parent materials in each geochemical region, together with enrichment and depletion processes of elements during weathering, have resulted in soils with specific properties and prerequisites for SOC stabilization against microbial decomposition (Table A3). In particular, stabilization mechanisms related to pedogenic oxides (Fig. 3) and the formation of organo–mineral associations are relevant for SOC stabilization at our sites, as illustrated by the strong correlation of variables representing organo–mineral complexes with SOC_{Bulk} and $\Delta^{14}C$ (Table 3). The influence of parent material geochemistry and weathering on the pattern of physically separated soil C fractions, in particular on stabilizing C in microaggregates, was smaller across soil geochemical regions than across soil depths. (Figs. 3 and 4 and Table 3). The most important variables for explaining m/s + c ratios were found to be soil depth, solid-phase mineralogy and the chemistry of the soil solution, which could in total explain 44 % of m/s + c variance (Table 2). We interpret the high m/s + c ratios in topsoils as indicative for the formation of stable microaggregates promoted by the higher abundance of C, which functions as a binding agent (Denef and Six, 2005) and the generally more fertile conditions in tropical topsoil compared to subsoil favoring microbial activity (Kidinda et al., 2020). The abundance of pedogenic oxides further promotes aggregation by providing reactive mineral surfaces (Oades, 1988). In this study, pedogenic oxides are determined by geochemistry with higher contents in mafic compared to felsic and mixed sedimentary soils (Fig. 3b). Therefore, mafic soils also stabilize more C in microaggregates. It is likely that the high amount of pedogenic oxides usually measured in microaggregates (Doetterl et al., 2015a) and the low amount of particulate organic matter (POM) measured in our study overall suggests that predominantly mineral-complexed SOC accumulated within the isolated aggregates. This is supported by studies showing that microaggregate-sized particles in deeply weathered tropical soils are rich in Fe and Al concretions (Cooper et al., 2005; Zotarelli et al., 2005; Denef et al. 2007; Martinez and Souza, 2020). Fe oxides like hematite can incorporate large amounts of Al in their crystal structure by substitution, especially within a kaolinite-rich soil matrix (Tardy and Nahon, 1985). Such (hydro)oxides of Al and Fe act as a cement-

ing agent in the formation of pseuosands, and their chemical composition is controlled by parent material geochemistry. In general, (hydro)oxides dominated by Fe are more abundant on mafic rocks, whereas Al is more abundant on rocks with low amounts of Fe (e.g., quartz-rich sedimentary rocks) (Martinez and Souza, 2020). In our study, both the parent material and soil geochemistry show considerable amounts of Al, even though the Fe content exceeds that of Al. The dominating soils are Ferralsols and Nitisols, which are dominated by kaolinitic clays. Given the above-mentioned observations, it is likely that Fe and Al concretions are present in the studied soils, even though the elemental composition of the concretions was not directly measured. In light of this finding, aggregation is an important means to promote the complexation of C with minerals (Martinez and Souza, 2020) but also the result of the tendency of pedogenic oxides to form stable aggregates (Doetterl et al., 2015a), which lends additional protection of soil C. When controlling for soil depth, our geochemical predictors ($rPC1_{nv}$, $rPC2_{nv}$, $rPC3_{nv}$, $rPC4_{nv}$) gained or retained similar prediction power (Table 3), showing the importance for predicting SOC target variables at all soil depths. Geochemical predictors were also more important to stabilize C in shallow and deep subsoils compared to topsoils, as indicated by the absence of correlations in topsoils but significant correlations in subsoils (data not shown).

4.2 Fossil organic carbon contributions to SOC_{bulk} and driving $\Delta^{14}C$

While depth trends in $\Delta^{14}C$ were similar across geochemical regions (Fig. 4a), soils developed on mixed sedimentary rocks were significantly depleted in $\Delta^{14}C$ for all topographic positions. A significant amount between 11.3 ± 2.6 and 52.0 ± 13.2 % FOC was found to contribute to SOC_{bulk} in soils developed on mixed sedimentary rocks (Table 1), thus supporting our initial hypothesis (iii) that FOC-bearing parent material will strongly impact SOC_{bulk}. Despite contributions of FOC of up to 52 %, SOC_{bulk} did not differ to the same extent between the geochemical regions (Fig. 4b). Two potential explanations could be found for this observation. First, fertility conditions and stabilization mechanisms against microbial decomposition in soils developed from mixed sedimentary parent material reduce the amount of SOC with modern biogenic origin drastically due to slower C cycling (Trumbore, 2009). However, neither $\Delta^{14}C$ nor the analyzed distribution of soil C fractions support this explanation. Biologically active topsoil $\Delta^{14}C$ in the mixed sediment region was less depleted than the subsoil counterparts when being compared across regions (Fig. 4). Additionally, auxiliary data on the overall net primary productivity of the investigated systems (Doetterl and Fiener, 2021a, b) point towards relatively comparable C inputs across the three regions, at least in topsoil. Subsoils of the sediment region, however, may receive significantly less C input, which is the subject of future investigations. A second explanation could be the decomposition of FOC once it enters more biologically active zones (i.e., topsoils), where climatic and edaphic conditions are more suitable for microbial decomposer communities. Findings on $\Delta^{14}C$ signatures of respired C indicate the presence of FOC contributing to CO_2 release (Bukombe et al., 2021). Here, on average only 6.7 ± 2.5 % of the respired CO_2 showed a fossil origin in the non-valley positions. Hence, the fact that FOC content increases with depth (Table 1) but is nearly depleted in topsoils indicates that these sources of fossil C, even though a poor source of nutrients and energy for microorganisms (Hemmingway et al., 2018), can become available to microbial decomposition under more suitable conditions. Statistically, differences in $\Delta^{14}C$ were best explained by soil depth (Table 2) but between regions by the presence of FOC in soils developed from mixed sedimentary parent material and when controlling for soil depth with geochemical variables (Table 3). Further, our model identified silt content as a strong predictor for $\Delta^{14}C$. It is possible that tropical soils form very stable silt-sized microaggregates (Six et al., 2000b), in which FOC is potentially stabilized. However, the low pedogenic oxide content in the mixed sedimentary region, important for microaggregate formation (Zotarelli et al., 2005; Denef et al., 2007; Doetterl et al., 2015a; Martinez and Souza, 2020), is not entirely supportive of this interpretation. There is also no statistically significant relationship between fine soil texture classes and the C associated with microaggregates or the free silt and clay fraction in our investigated sites in the sediment region (data not shown). We argue, therefore, that no mechanistic relationship exists between $\Delta^{14}C$ and silt content, and the observed relationship is to be interpreted as an autocorrelation between the high amounts of ^{14}C-depleted FOC in the mixed sedimentary region and the fact that these sediments have a higher silt content than their felsic and mafic counterparts.

4.3 Interpreting soil controls for predicting SOC dynamics

Our regression analyses revealed that a wide variety of soil variables contribute to predicting SOC and its turnover in a quantitative and qualitative way (Tables 2 and A4). An exact mechanistic interpretation is difficult due to the relatively small number of observations compared to potential predictor variables. However, in general a set of variables related to soil fertility and the chemistry of the solid phase and soil solution contributed to predicting our three target variables: (1) SOC_{bulk}, (2) $\Delta^{14}C$ and (3) m/s+c (Tables 2 and A4). Furthermore, some interpretation of the included rotated components is possible because their respective loading is clearly distinct from each other (Table A4, Fig. 5). Notably, the prediction power of our models was dominated by soil depth (Table 2) for all three target variables. However, partial correlation revealed that soil depth covered relationships between the target variables and our predictors (Table 3), indicating

that soil depth is autocorrelated with variability in soil mineralogy and soil fertility. For example, solid-phase mineralogy and organo–mineral complexes reflect the amount of total elements in the soil and their transformation into secondary minerals and thus the amount of reactive mineral surfaces, which are highly relevant in the sorptive protection of SOC (Oades, 1984; Evanko and Dzombak, 1998; Kleber et al., 2015). Similarly, the chemistry of the soil solution represents properties that are relevant for C stabilization against microbial decomposition. Here, low pH levels can mobilize Al^{3+}, which eventually sorbs onto reactive mineral surfaces, preventing C stabilization (Smith, 1999). In our mafic soils, sorptive C stabilization created by pedogenic oxides leads to high SOC_{bulk} (Figs. 3 and 4 and Table 2) and supports the formation of aggregates. Conversely, felsic soils are low in pedogenic oxides and thus have low sorption potential and consequently also the lowest SOC_{bulk}. Clay content, identified as a major factor for stabilizing SOC in temperate soils (Angst et al., 2018) and also in tropical soil systems (Quesada et al., 2020; Souza et al., 2017), was not identified as a major control for our soils. This illustrates the importance of understanding soil geochemical preconditions when identifying controls of C dynamics and that findings are not necessarily transferable, even between comparable soil types and climates. Overall, we found that chemical stabilization of SOC, especially by organo–mineral complexation, contributed the most to explaining differences in SOC_{bulk} in the analyzed soils, while aggregation, profiting from the abundance of pedogenic oxides and stable Fe and Al structures in soils, added additional C stabilization potential. Hence, under similar climatic conditions and similar C input through vegetation (Doetterl et al., 2021b), our data indicate that C stabilization mechanisms in soil control SOC stocks and turnover in deeply tropical weathered soils more so than soil fertility conditions and drive patterns of SOC stocks across geochemical regions (Figs. 3 an 4). Our results are comparable to other studies investigating the impact of reactive mineral surfaces on SOC_{bulk} in tropical kaolinitic soils (Bruun et al., 2010) and the importance of sorptive processes to C on mineral surfaces (Jagadamma et al., 2014). These processes have been identified to be important for soil C stabilization in a variety of ecosystems and climate zones (Murphy et al., 1992; Evanko and Dzombak, 1998; Kögel-Knabner et al., 2008; Fang et al., 2019). However, they stand out in tropical soils due to the high amounts of Fe and Al oxides in the system overall and the advanced stage of weathering of soils that led to the formation of low-activity clays and other end-member minerals with low potential for C sorption (Ito and Wagai, 2017).

5 Conclusions and outlook

Overall, we found a minimal impact of topography on SOC variables as a function of soil fluxes along slopes but observed higher SOC stocks in valleys compared to non-valley positions due to varying hydrological conditions and alluvial processes. Instead, chemical soil properties, derived from parent material geochemistry, were identified as major explanatory factors. We argue that the strong role of geochemical variables in explaining SOC is a function of reactive mineral surfaces dependent on the composition of the parent material and its weathering status. More available reactive surfaces will favor sorptive C stabilization and the formation of stable aggregates, thus leading to higher SOC_{bulk}. In the deeply weathered tropical soil systems investigated, the formation of organo–mineral complexes of Al, Fe and Mn was most important for explaining SOC_{bulk} across geochemical regions, and the impact of clay content was minimal. Differences in the relative abundance of C associated with microaggregates and with free silt and clay fractions differed significantly between geochemical regions and soil depth, indicating that despite long-lasting weathering, mafic soils can protect C better than their felsic and mixed sediment counterparts. Aggregate formation in tropical soils seems to profit from the abundance of pedogenic oxides in soils, linking two of the most important mineral-related C stabilization mechanisms against microbial decomposition in soil with geochemical variability retained from parent material. Differences in $\Delta^{14}C$ were best explained by soil depth as a proxy for factors limiting microbial respiration, which are more pronounced in subsoils than in topsoils. While following similar depth trends, the presence of fossil organic carbon contributed to significantly explain the $\Delta^{14}C$ pattern when comparing across regions. It is recommended to repeat our analyses in other tropical soil and land use systems, where external drivers such as soil redistribution, weathering stages or stabilization mechanisms against microbial decomposition might differ. This way, a more spatially explicit picture of C stabilization mechanisms will contribute to understanding future tropical SOC dynamics in light of ongoing climatic and land use changes, as well as the representation of SOC stabilization and destabilization in land surface models.

Appendix A

Table A1. Partial correlation analysis between SOC_{bulk} and climate variables (Fick and Hijams, 2017) controlling for geochemical soil properties. Zero-order correlation displays the Pearson r values when including no control variables. The controlled correlation shows the Pearson r value when controlling for DCB-extractable oxides of Al, Fe and Mn, exchangeable bases and total P.

Soil depth [cm]	Control variables	MAP	MAT	PET
0–10	zero-order	−0.17	0.00	−0.08
	DCB-extr. oxides (Al, Fe, Mn), exchangeable bases, total P	−0.16	−0.26	−0.40
30–40	zero-order	0.67[a]	−0.90[b]	−0.93[b]
	DCB-extr. oxides (Al, Fe, Mn), exchangeable bases, total P	−0.56	−0.03	−0.43
60–70	zero-order	−0.06	−0.24	−0.33
	DCB-extr. oxides (Al, Fe, Mn), exchangeable bases, total P	0.00	−0.13	−0.14

[a] $p < 0.05$; [b] $p < 0.001$.

https://doi.org/10.5194/soil-7-453-2021

Table A2. SOC variables grouped by soil depth, topographic position and geochemical regions (section 1: mafic; section 2: felsic; section 3: mixed). Different capital letters indicate significant differences in means ($p < 0.05$).

Section 1: mafic magmatic										
		0–10 cm			30–40 cm			60–70 cm		
Parameter	Unit	Plateau	Sloping	Valley	Plateau	Sloping	Valley	Plateau	Sloping	Valley
C	mass%	8.54 ± 3.37 *	5.4 ± 0.59 *	8.62 ± 1.11 *	2.11 ± 0.02 *	2.55 ± 0.32 *	3.8 ± 0.66 *	1.42 ± 0.27 *	2.02 ± 0.92 *	2.62 ± 0.72 *
N	mass%	0.7 ± 0.19 *	0.55 ± 0.06 *	0.87 ± 0.12 *	0.21 ± 0.01 A	0.25 ± 0.02 A	0.38 ± 0.05 B	0.15 ± 0.01 *	0.2 ± 0.1 *	0.25 ± 0.04 *
C/N	–	11.78 ± 1.89 *	9.75 ± 0.68 *	9.92 ± 0.78 *	10.17 ± 0.23 *	10.26 ± 0.76 *	10.14 ± 1.24 *	9.61 ± 0.99 *	10.18 ± 0.92 *	10.52 ± 2.32 *
SOC_{bulk}	$tC\,ha^{-1}$	65.63 ± 25.9 *	43.07 ± 6.6 *	62.24 ± 11.41 *	25.02 ± 0.24 A	29.98 ± 3.22 A	41.22 ± 4.6 B	17.2 ± 3.2 *	25.78 ± 12.06 *	32.19 ± 9.15 *
m/s + c	–	1.43 ± 0.3 *	1.41 ± 0.45 *	1.72 ± 0.83 *	1.3 ± 0.08 *	1.13 ± 0.28 *	1.66 ± 0.5 *	1.11 ± 0.11 *	0.98 ± 0.15 *	1.66 ± 1.06 *
$SOC_{>250\,\mu m}$	%	5.09 ± 2.37 *	3.62 ± 1.14 *	4.12 ± 3.38 *	1.48 ± 0.33 *	1.36 ± 0.42 *	2.18 ± 1.57 *	1.32 ± 0.03 *	1.31 ± 1.01 *	2.12 ± 1.04 *
$SOC_{53-250\,\mu m}$	%	55.3 ± 3.38 *	55.2 ± 9.49 *	57.9 ± 12.83 *	55.63 ± 1.59 *	51.52 ± 7.26 *	60.28 ± 7.44 *	51.7 3 ± 2.54 *	48.61 ± 3.83 *	56.98 ± 16.71 *
$SOC_{<53\,\mu m}$	%	39.61 ± 5.75 *	41.18 ± 8.52 *	37.98 ± 13.96 *	42.89 ± 1.47 *	47.12 ± 6.93 *	37.54 ± 6.03 *	46.95 ± 2.51 *	50.08 ± 3.76 *	40.91 ± 15.67 *
Section 2: felsic magmatic										
		0–10 cm			30–40 cm			60–70 cm		
Parameter	Unit	Plateau	Sloping	Valley	Plateau	Sloping	Valley	Plateau	Sloping	Valley
C	mass%	4.58 ± 1.14 *	3.39 ± 0.79 *	2.99 ± 0.39 *	0.95 ± 0.07 *	0.87 ± 0.21 *	0.55 ± 0.13 *	0.55 ± 0.08 *	0.51 ± 0.12 *	0.28 ± 0.11*
N	mass%	0.45 ± 0.08 *	0.35 ± 0.07 *	0.29 ± 0.03 *	0.1 ± 0.01 *	0.09 ± 0.02 *	0.06 ± 0.01 *	0.06 ± 0.01 *	0.05 ± 0.01 *	0.03 ± 0.02*
C/N	–	10.18 ± 0.65 *	9.77 ± 0.62 *	10.31 ± 1.98 *	10.29 ± 0.04 *	10.31 ± 1.81 *	10.37 ± 0.52 *	9.57 ± 0.04 *	10.6 ± 2 *	9.89 ± 1.55 *
SOC_{bulk}	$tC\,ha^{-1}$	46.75 ± 28.49 *	44.08 ± 9.72 *	40.42 ± 8.03 *	16.41 ± 2.87 *	15.81 ± 4.61 *	9.88 ± 2.25 *	9.03 ± 1.05 *	10.32 ± 2.96 *	5.95 ± 3.26 *
m/s + c	–	1.23 ± 0.54 AB	1.37 ± 0.47 B	2.45 ± 0.39 A	0.68 ± 0.01 *	1.11 ± 0.37 *	0.72 ± 0.07 *	1.06 ± 0.28 *	1.13 ± 0.62 *	0.53 ± 0.13 *
$SOC_{>250\,\mu m}$	%	12.77 ± 6.31 *	10.15 ± 3.84 *	12.57 ± 7.94 *	5.62 ± 2.66 *	9.43 ± 9.97 *	3.71 ± 1.6 *	3.41 ± 0.47 *	8.26 ± 7.71 *	4.88 ± 2.37 *
$SOC_{53-250\,\mu m}$	%	46.52 ± 6.42 *	50.49 ± 7.8 *	61.96 ± 7.91 *	38.14 ± 1.41 *	46.34 ± 9.4 *	40.16 ± 2.9 *	49.31 ± 6.29 *	45.34 ± 15.37 *	32.94 ± 5.73*
$SOC_{<53\,\mu m}$	%	40.71 ± 12.73 AB	39.36 ± 8.45 A	25.47 ± 2.23 B	56.24 ± 1.25 *	44.22 ± 9.51 *	56.13 ± 1.47 *	47.28 ± 6.75 *	46.4 ± 14.02 *	62.18 ± 3.38 *
Section 3: mixed sedimentary rocks										
		0–10 cm			30–40 cm			60–70 cm		
Parameter	Unit	Plateau	Sloping	Valley	Plateau	Sloping	Valley	Plateau	Sloping	Valley
C	mass%	6.95 ± 0.46 *	4.83 ± 1.91 *	6.3 ± 3.05 *	2.42 ± 0.15 *	2.41 ± 1.06 *	1.63 ± 0.78 *	1.36 ± 0.26 *	1.78 ± 0.86 *	2.28 ± 2.14 *
N	mass%	0.47 ± 0.06 *	0.31 ± 0.13 *	0.37 ± 0.18 *	0.15 ± 0.01 *	0.14 ± 0.07 *	0.06 ± 0.03 *	0.09 ± 0.01 *	0.09 ± 0.07 *	0.06 ± 0.05 *
C/N	–	14.84 ± 0.98 *	15.85 ± 1.86 *	17.04 ± 0.73 *	15.63 ± 1.46 A	18.63 ± 4.71 A	27.15 ± 2.98 B	15.55 ± 0.99 *	33.41 ± 37.42 *	30.29 ± 17.28 *
SOC_{bulk}	$tC\,ha^{-1}$	48.41 ± 6.59 *	41.71 ± 8.47 *	52.75 ± 30.72 *	31.08 ± 3.33 *	30.06 ± 7.42 *	26.88 ± 15.82 *	20.2 ± 4.26 *	25.74 ± 11.29 *	40.86 ± 38.35 *
m/s + c	–	0.9 ± 0.66 *	0.94 ± 0.31 *	2.97 ± 2.43 *	0.53 ± 0.08 *	0.8 ± 0.34 *	1.12 ± 0.59 *	0.85 ± 0.2 *	0.7 ± 0.69 *	1.15 ± 0.59 *
$SOC_{>250\,\mu m}$	%	6.74 ± 3.98 *	6.43 ± 7.14 *	22.19 ± 12.29 *	13.37 ± 19.44 *	6.26 ± 1.72 *	15.09 ± 9.18 *	4.41 ± 3.8 *	6.37 ± 4.6 *	10.42 ± 11.4 *
$SOC_{53-250\,\mu m}$	%	40.18 ± 15.39 *	44.7 ± 9.46 *	52.71 ± 6.82 *	30.22 ± 8.01 *	40.16 ± 9.54 *	42.34 ± 6.19 *	43.28 ± 3.52 *	27.31 ± 20.91 *	44.56 ± 9.71 *
$SOC_{<53\,\mu m}$	%	53.07 ± 17.58 *	48.87 ± 6.1 *	25.11 ± 14.87 *	56.4 ± 12.28 *	53.59 ± 8.99 *	42.57 ± 13.79 *	52.3 ± 7.28 *	49.65 ± 30.66 *	45.02 ± 18.14 *

Asterisks indicate no significant differences in means ($p > 0.05$). Means are compared across topographical positions for each depth increment in each geochemical region (plateau $n = 3$, slopes $n = 6$, valley $n = 3$).

Table A3. Absolute and relative differences of mineral soil at plateau positions (30–40 cm soil depth) compared to parent material. Maximum and minimum values refer to the maximum and minimum depletion, respectively. If sample size was $n = 1$, the corresponding standard deviation was not applicable (n/a).

		Mafic		Felsic		Mixed	
		Soil absolute difference [ppm]	Relative difference Δ [%]	Soil absolute difference [ppm]	Relative difference Δ [%]	Soil absolute difference [ppm]	Relative difference Δ [%]
Ca	Mean ± SD	−5765 ± 5814	−99 ± 101	1443 ± n/a	1240 ± n/a	−55 ± 95	−100 ± 172
	Max	−12 937	−100	1028	194	−164	−100
	Min	−75	−38	1559	n/a	0	n/a
K	Mean ± SD	161 ± 970	20 ± 603	1148 ± n/a	618 ± n/a	−248 ± 566	−32 ± 228
	Max	−1621	−65	743	126	−774	−62
	Min	984	2687	1318	8790	499	306
Mg	Mean ± SD	−10 414 ± 3417	−83 ± 33	1160 ± n/a	1015 ± n/a	587 ± 211	527 ± 36
	Max	−14 333	−87	718	129	341	179
	Min	−5488	−72	1274	n/a	876	2235
Na	Mean ± SD	−519 ± 850	−63 ± 164	148 ± n/a	677 ± n/a	43 ± 59	92 ± 138
	Max	−1954	−90	102	149	−34	−53
	Min	313	375	163	2414	117	834
P	Mean ± SD	−2133 ± 1361	−58 ± 64	403 ± n/a	746 ± n/a	585 ± 201	289 ± 34
	Max	−3774	−72	223	96	333	89
	Min	186	14	450	6671	874	2583
Fe	Mean ± SD	28 849 ± 25 496	32 ± 88	30 867 ± n/a	284 ± n/a	87 917 ± 24 429	379 ± 28
	Max	−6967	−6	−12 878	−24	56 114	157
	Min	60 099	85	39 115	1482	12 1456	3486
Al	Mean ± SD	24 730 ± 37 287	39 ± 151	25 226 ± n/a	487 ± n/a	49 252 ± 5537	799 ± 11
	Max	−33 553	−32	−9013	−23	41 728	383
	Min	78 824	307	29 966	6859	55 961	1514
Mn	Mean ± SD	2040 ± 1461	160 ± 72	1251 ± n/a	3126 ± n/a	168 ± 48	776 ± 29
	Max	584	34	1125	675	91	168
	Min	3273	308	1291	n/a	213	17 591
Si	Mean ± SD	−16 700 ± n/a	−12 ± n/a	−21 6070 ± n/a	−58 ± n/a	−24 1033 ± n/a	−67 ± n/a
	Max	−46 000	−27	−25 6000	−62	−29 8700	−71
	Min	9500	8	−55 900	−26	−16 3000	−58

Table A4. Rotated principal components and variable loadings of varimax-rotated principal component analysis for non-valley positions (rPC) ($n = 27$). Variable loadings of Pearson's $r > 0.5$ and < -0.5 are highlighted with bold font type. The following variables contributed to the components: to describe the total element content in the soils (associated with $rPC1_{nv}$ and $rPC4_{nv}$), the total reserve in base cations (TRB; sum of total Mg, Ca, K and Na), total P, metals (sum of total Fe, Al and Mn) and total Si were used. Pyrophosphate-, oxalate- and DCB-extractable phases of Al, Fe and Mn characterize the pedogenic oxides. Exchangeable acidity and bases, effective cation exchange capacity (ECEC) base saturation, CEC base saturation, pH_{KCL} and bio-available P (bray-P) reflect soil fertility (associated with $rPC2_{nv}$). The ratio of pH/clay, ECEC base saturation/clay and CEC base saturation/clay are proxies for clay activity (associated with $rPC2_{nv}$). Clay, silt and sand describe the texture (associated with $rPC1_{nv}$ and $rPC3_{nv}$), and several weathering indices (Al_{DCB}/Al_t ratio, Fe_{DCB}/Fe_t ratio, Al/Si ratio, Fe/Si ratio, Ca/Ti ratio and the chemical index of alteration, CIA) characterize the soil weathering stage (predominantly associated with $rPC1_{nv}$). SOC_{litter}, $SOC_{organic}$ and root input describe the C input (associated with $rPC2_{nv}$ and $rPC3_{nv}$).

			$rPC1_{nv}$	$rPC2_{nv}$	$rPC3_{nv}$	$rPC4_{nv}$
	Eigenvalue		9.34	9.15	1.82	1.57
	Proportion var. (%)		0.33	0.33	0.07	0.06
	Cumulative var. (%)		0.33	0.66	0.73	0.78
	Mechanistic interpretation		solid-phase mineralogy	chemistry of the soil solution	silt content	organo–mineral complexes
	Total elements					
1	TRB	mass%	0.39	**0.83**	∼0	−0.12
2	total P	mass%	**0.83**	∼0	−0.21	∼0
3	metals ($\sum$ total Fe, total Al, total Mn)	mass%	**0.95**	−0.24	∼0	∼0
4	total Si	mass%	**−0.80**	∼0	−0.38	−0.32
	Pedogenic oxides					
5	pyro.-extr. Fe, Al, Mn	mass%	∼0	−0.39	∼0	**0.82**
6	oxalate-extr. Fe, Al, Mn	mass%	**0.88**	−0.26	∼0	0.31
7	DCB-extr. Fe, Al, Mn	mass%	**0.95**	−0.19	∼0	−0.13
	Soil fertility					
8	exchangeable acidity	me/100 g	0.31	**−0.65**	−0.13	0.27
9	exchangeable bases	me/100 g	−0.15	**0.96**	∼0	∼0
10	ECEC base saturation	%	−0.20	**0.79**	0.33	−0.23
11	CEC base saturation	%	−0.38	**0.87**	0.21	−0.17
12	soil pH (KCl)	–	−0.24	**0.82**	0.21	∼0
13	bio available P (bray)	$mg\,kg^{-1}$	0.23	**0.50**	0.14	∼0
	Clay activity					
14	pH/clay	–	**−0.73**	**0.66**	∼0	∼0
15	ECEC base saturation/clay	–	−0.33	**0.83**	0.27	−0.17
16	CEC base saturation/clay	–	−0.41	**0.87**	0.15	−0.12
	Texture					
17	clay	%	**0.89**	−0.24	∼0	∼0
18	silt	%	−0.14	−0.39	**−0.89**	∼0
19	sand	%	**−0.76**	0.42	0.37	∼0
	Weathering					
20	Al_{DCB}/Al_t	–	−0.29	∼0	0.11	−0.12
21	Fe_{DCB}/Fe_t	–	**0.65**	∼0	∼0	0.27
22	Al/Si	–	**0.94**	∼0	0.19	−0.12
23	Fe/Si	–	**0.91**	−0.25	∼0	0.17
24	Ca/Ti	–	−0.25	**0.90**	∼0	∼0
25	CIA	%	0.44	**−0.84**	∼0	∼0
	C input					
26	SOC_{litter}	$t\,C\,ha^{-1}$	−0.26	0.19	∼0	−0.20
27	$SOC_{organic}$	$t\,C\,ha^{-1}$	−0.27	**−0.59**	**−0.53**	0.46
28	root input	$kg\,m^{-3}$	−0.28	**0.52**	−0.17	0.23

Data availability. All data used in this study will be published in an open access project-specific database https://doi.org/10.5880/fidgeo.2021.009 (Doetterl et al., 2021b). The specific data of this publication is available upon request from the corresponding author.

Sample availability. All soil samples are logged and barcoded at the Department of Environmental Science at ETH Zurich, Switzerland.

Supplement. The supplement related to this article is available online at: https://doi.org/10.5194/soil-7-453-2021-supplement.

Author contributions. SD and PF designed the research. MR conducted the sampling campaign and collected the data. All authors analyzed and interpreted the data. All authors contributed to the writing of the paper.

Competing interests. Sebastian Doetterl is a liaison editor of the special issue "Tropical biogeochemistry of soils in the Congo Basin and the African Great Lakes region", and Johan Six is an executive editor and Peter Fiener a topical editor of *SOIL*. However, none of them were involved in the review process of this paper. All the other authors declare that they have no conflict of interest.

Disclaimer. Publisher's note: Copernicus Publications remains neutral with regard to jurisdictional claims in published maps and institutional affiliations.

Special issue statement. This article is part of the special issue "Tropical biogeochemistry of soils in the Congo Basin and the African Great Lakes region". It is not associated with a conference.

Acknowledgements. This work is part of the DFG funded Emmy Noether Junior Research Group "Tropical soil organic carbon dynamics along erosional disturbance gradients in relation to soil geochemistry and land use" (TROPSOC; project no. 387472333). The authors like to thank following collaborators of this project: International Institute of Tropical Agriculture (IITA), Max Planck Institute for Biogeochemistry, Institute of Soil Science and Site Ecology at Technical University Dresden, Sustainable Agroecosystems Group and the Soil Resources Group both located at ETH Zurich and the Faculty of Agriculture at the Catholic University of Bukavu. The authors would like to thank the whole TROPSOC team, especially the student assistants, for their important work in the laboratory and all fieldwork helpers, who made the sampling campaign possible. The authors like to thanks the three anonymous referees for their valuable comments.

Financial support. This research has been supported by the Deutsche Forschungsgemeinschaft (grant no. 387472333).

Review statement. This paper was edited by Pauline Chivenge and reviewed by three anonymous referees.

References

Angst, G., Messinger, J., Greiner, M., Häusler, W., Hertel, D., Kirfel, K., Kögel-Knabner, I., Leuschner, C., Rethemeyer, J., and Mueller, C. W.: Soil organic carbon stocks in topsoil and subsoil controlled by parent material, carbon input in the rhizosphere, and microbial-derived compounds, Soil Biol. Biochem., 122, 19–30, https://doi.org/10.1016/j.soilbio.2018.03.026, 2018.

Allison, S. D. and Vitousek, P. M.: Responses of extracellular enzymes to simple and complex nutrient inputs, Soil Biol. Biochem., 37, 937–944, https://doi.org/10.1016/j.soilbio.2004.09.014, 2005.

Bascomb, C. L.: Distribution of pyrophosphate-extractable iron and organic carbon in soils of various groups, J. Soil Sci., 19, 251–268, https://doi.org/10.1111/j.1365-2389.1968.tb01538.x, 1968.

Berhe, A. A., Harte, J., Harden, J. W., and Torn, M. S.: The significance of the erosion-induced terrestrial carbon sink, BioScience, 57, 337–346, https://doi.org/10.1641/B570408, 2007.

Berhe, A. A., Harden, J. W., Torn, M. S., Kleber, M., Burton, S. D., and Harte, J.: Persistence of soil organic matter in eroding versus depositional landform positions, J. Geophys. Res., 117, 1–16, https://doi.org/10.1029/2011JG001790, 2012.

Blagodatskaya, E., Blagodatsky, S., Khomyakov, N., Myachina, O., and Kuzyakov, Y.: Temperature sensitivity and enzymatic mechanisms of soil organic matter decomposition along an altitudinal gradient on Mount Kilimanjaro, Sci. Rep.-UK, 6, 1–11, https://doi.org/10.1038/srep22240, 2016.

Bruun, T. B., Elberling, B., and Christensen, B. T.: Lability of soil organic carbon in tropical soils with different clay minerals, Soil Biol. Biochem., 42, 888–895, https://doi.org/10.1016/j.soilbio.2010.01.009, 2010.

Bukombe, B., Fiener, P., Hoyt, A. M., and Doetterl, S.: Controls on heterotrophic soil respiration and carbon cycling in geochemically distinct African tropical forest soils, SOIL Discuss. [preprint], https://doi.org/10.5194/soil-2020-96, in review, 2021.

Cerri, C., Feller, C., Balesdent, J., Victoria, R., and Plenecassagne, A.: Application du traçage isotopique naturel en ^{13}C, à l'étude de la dynamique de la matière organique dans les sols, C. R. Acad. Sci. II, 300, 423–427, 1985.

Chenu, C. and Plante, A. F.: Clay-sized organo-mineral complexes in a cultivation chronosequence: revisiting the concept of the 'primary organo-mineral complex', Eur. J. Soil Sci., 57, 596–607, https://doi.org/10.1111/j.1365-2389.2006.00834.x, 2006.

Cooper, M., Vidal-Torrado, P., and Chaplot, V.: Origin of microaggregate in soils with ferralic horizons, Scienta Agricola, 62, 256–263, https://doi.org/10.1590/S0103-90162005000300009, 2005.

Cotrufo, M. F., Wallenstein, M. D., Boot, C. M., Denef, K., and Paul, E.: The microbial efficiency-matrix stabilization (MEMS) framework integrates plant litter decomposition with soil organic matter stabilization: do labile plant inputs form sta-

ble soil organic matter?, Glob. Change Biol., 19, 988–995, https://doi.org/10.1111/gcb.12113, 2013.

Czimczik, C. I. and Masiello, C. A.: Controls on black carbon storage in soils, Global Biogeochem. Cy., 21, 1–8, https://doi.org/10.1029/2006GB002798, 2007.

Dahlgren, R. A.: Quantification of allophane and imogolite, quantitative methods in soil mineralogy, in: Quantitative Methods in Soil Mineralogy, edited by: Chairs, J. E. and Stucki, J. W., Soil Sci. Soc. Am. J., Madison, Wisconsin, USA, 430–451, 1994.

Davidson, E. A. and Janssens, I. A.: Temperature sensitivity of soil carbon decomposition and feedbacks to Climate Change, Nature, 440, 165–173, https://doi.org/10.1038/nature04514, 2006.

Day, R. W. and Quinn, G. P.: Comparisons of treatments after an analysis of variance in ecology, Ecol. Monogr., 59, 433–463, https://doi.org/10.2307/1943075, 1989.

Denef, K. and Six, J.: Clay mineralogy determines the importance of biological versus abiotic processes for macroaggregate formation and stabilization, Eur. J. Soil Sci., 56, 469–479, https://doi.org/10.1111/j.1365-2389.2004.00682.x, 2005.

Denef, K. and Six, J.: Contributions of incorporated residue and living roots to aggregate-associated and microbial carbon in two soils with different clay mineralogy, Eur. J. Soil Sci., 57, 774–786, https://doi.org/10.1111/j.1365-2389.2005.00762.x, 2006.

Denef, K., Six, J., Merckx, R., and Paustian, K.: Carbon sequestration in microaggregates of no-tillage soils with different clay mineralogy, Soil Sci. Soc. Am. J., 68, 1935–1944, https://doi.org/10.2136/sssaj2004.1935, 2004.

Denef, K., Zotarelli, L., Boddey, R. M., and Six, J.: Microaggregate-associated carbon as a diagnostic fraction for management-induced changes in soil organic carbon in two Oxisols, Soil Biol. Biochem., 5, 1165–1172, https://doi.org/10.1016/j.soilbio.2006.12.024, 2007.

Detto, M., Muller-Landau, H. C., Mascaro, J., and Asner, G. P.: Hydrological networks and associated topographic variation as templates for the spatial organization of tropical forest vegetation, PloS One, 8, 1–13, https://doi.org/10.1371/journal.pone.0076296, 2013.

Doetterl, S., Cornelis, J.-T., Six, J., Bodé, S., Opfergelt, S., Boeckx, P., and Van Oost, K.: Soil redistribution and weathering controlling the fate of geochemical and physical carbon stabilization mechanisms in soils of an eroding landscape, Biogeosciences, 12, 1357–1371, https://doi.org/10.5194/bg-12-1357-2015, 2015a.

Doetterl, S., Stevens, A., Six, J., Merckx, R., van Oost, K., Pinto, M. C., Casanova-Katny, A., Muñoz, C., Boudin, M., Venegas, E. Z., and Boeckx, P.: Soil carbon storage controlled by interactions between geochemistry and climate, Nat. Geosci., 8, 780–783, https://doi.org/10.1038/ngeo2516, 2015b.

Doetterl, S., Berhe, A. A., Nadeu, E., Wang, Z., Sommer, M., and Fiener, P.: Erosion, deposition and soil carbon: a review of process-level controls, experimental tools and models to address C cycling in dynamic landscapes, Earth-Sci. Rev., 154, 102–122, https://doi.org/10.1016/j.earscirev.2015.12.005, 2016.

Doetterl, S., Berhe, A. A., Arnold, C., Bodé, S., Fiener, P., Finke, P., Fuchslueger, L., Griepentrog, M., Harden, J. W., Nadeu, E., Schnecker, J., Six, J., Trumbore, S., van Oost, K., Vogel, C., and Boeckx, P.: Links among warming, carbon and microbial dynamics mediated by soil mineral weathering, Nat. Geosci., 11, 589–593, https://doi.org/10.1038/s41561-018-0168-7, 2018.

Doetterl, S., Asifiwe, R., Baert, G., Bamba, F., Bauters, M., Boeckx, P., Bukombe, B., Cadisch, G., Cooper, M., Cizungu, L., Hoyt, A., Kabaseke, C., Kalbitz, K., Kidinda, L., Maier, A., Mainka, M., Mayrock, J., Muhindo, D., Mujinya, B., Mukotanyi, S., Nabahungu, L., Reichenbach, M., Rewald, B., Six, J., Stegmann, A., Summerauer, L., Unseld, R., Vanlauwe, B., Van Oost, K., Verheyen, K., Vogel, C., Wilken, F., and Fiener, P.: Organic matter cycling along geochemical, geomorphic and disturbance gradients in forests and cropland of the African Tropics – Project TropSOC Database Version 1.0, Earth Syst. Sci. Data Discuss. [preprint], https://doi.org/10.5194/essd-2021-73, in review, 2021a.

Doetterl, S., Bukombe, B., Cooper, M., Kidinda, L., Muhindo, D., Reichenbach, M., Stegmann, A., Summerauer, L., Wilken, F., and Fiener, P.: TropSOC Database, Version 1.0. GFZ Data Services [data set], Helmholtz Centre Potsdam – GFZ German Research Centre for Geosciences Public Law Foundation, Potsdam, Germany, https://doi.org/10.5880/fidgeo.2021.009, 2021b.

Dove, N. C., Arogyaswamy, K., Billings, S. A., Botthoff, J. K. Carey, C. J. Caitlin, C., DeForest, J. L., Dawson, F., Fierer, N., Gallery, R. E., Kaye, J. P., Lohse, K. A., Maltz, M. R., Mayorga, E., Pett-Ridge, J., Yang, W. H., Hart, S. C., and Aronson, E. L.: Continental-scale patterns of extracellular enzyme activity in the subsoil: an overlooked reservoir of microbial activity, Environ. Res. Lett., 15, 1040a1, https://doi.org/10.1088/1748-9326/abb0b3, 2020.

Eusterhues, K., Rumpel, C., Kleber, M., and Kögel-Knabner, I.: Stabilisation of soil organic matter by interactions with minerals as revealed by mineral dissolution and oxidative degradation, Org. Geochem., 34, 1591–1600, https://doi.org/10.1016/j.orggeochem.2003.08.007, 2003.

Evanko, C. R. and Dzombak, D. A.: Influence of structural features on sorption of NOM-analoque organic acids to goethite, Environ. Sci. Technol., 32, 2846–2855, https://doi.org/10.1021/es980256t, 1998.

Fang, K., Qin, S., Chen, L., Zhang, Q., and Yang, Y.: Al/Fe mineral controls on soil organic carbon stock across Tibetan alpine grasslands, J. Geophys. Res.-Biogeo., 124, 247–259, https://doi.org/10.1029/2018JG004782, 2019.

FAO: Guidelines for soil description, 4th edn.,, available at http://www.fao.org/3/a-a0541e.pdf (last access: 15 June 2021), FAO, Rome, 2006.

FAO: World references base for soil resources 2014. International soil classification system for naming soils and creating legends for soil maps, Update 2015, Food and Agriculture Organization of the United Nations, Rome, Italy, 203 pp., 2014.

Feng, W., Liang, J., Hale, L. E., Jung, C. G., Chen, J., Zhou, J., Xu, M., Yuan, M., Wu, L., Bracho, R., Pegoraro, E., Schuur, E. A. G., and Luo, Y.: Enhanced decomposition of stable soil organic carbon and microbial catabolic potentials by long-term field warming, Glob. Change Biol., 23, 4765–4776, https://doi.org/10.1111/gcb.13755, 2017.

Fiantis, D., Nelson, M., Shamshuddin, J., Goh, T. B., and van Ranst, E.: Determination of the geochemical weathering indices and trace elements content of new volcanic ash deposits from Mt. Talang (West Sumatra) Indonesia, Eurasian Soil Sci.+, 43, 1477–1485, https://doi.org/10.1134/S1064229310130077, 2010.

Fick, S. E. and Hijmans, R. J.: WorldClim 2: new 1-km spatial resolution climate surfaces for global land areas, Int. J. Climatol., 37, 4302–4315, https://doi.org/10.1002/joc.5086, 2017.

Finke, P. A. and Hutson, J. L.: Modelling soil genesis in calcareous loess, Geoderma, 145, 462–479, https://doi.org/10.1016/j.geoderma.2008.01.017, 2008.

Fontaine, S., Bardoux, G., Abbadie, L., and Mariotti, A.: Carbon input to soil may decrease soil carbon content, Ecol. Lett., 7, 314–320, https://doi.org/10.1111/j.1461-0248.2004.00579.x, 2004.

Gregorich, E. G., Greer, K. J., Anderson, D. W., and Liang, B. C.: Carbon distribution and losses: erosion and deposition effects, Soil Till. Res., 47, 291–302, https://doi.org/10.1016/S0167-1987(98)00117-2, 1998.

Grömping, U.: Relative importance for linear regression in R: the package relaimpo, J. Stat. Softw., 17, 1–27, https://doi.org/10.18637/jss.v017.i01, 2006.

Harden, J. W., Sharpe, J. M., Parton, W. J., Ojima, D. S., Fries, T. L., Huntington, T. G., and Dabney, S. M.: Dynamic replacement and loss of soil carbon on eroding cropland, Global Biogeochem. Cy., 13, 885–901, https://doi.org/10.1029/1999GB900061, 1999.

Hemingway, J. D., Hilton, R. G., Hovius, N., Eglinton, T. I., Haghipour, N., Wacker, L., Chen, M.-C., and Galy, V. V.: Microbial oxidation of lithospheric organic carbon in rapidly eroding tropical mountain soils, Science, 360, 209–212, https://doi.org/10.1126/science.aao6463, 2018.

IBM: SPSS Statistics for Windows, IBM Corp., 2019.

Ito, A. and Wagai, R.: Data descriptor: global distribution of clay-size minerals on land surface for biogeochemical and climatological studies, Sci. Data, 4, 1–11, https://doi.org/10.1038/sdata.2017.103, 2017.

Jagadamma, S., Mayes, M. A., Zinn, Y. L., Gísladóttir, G., and Russell, A. E.: Sorption of organic carbon compounds to the fine fraction of surface and subsurface soils, Geoderma, 213, 79–86, https://doi.org/10.1016/j.geoderma.2013.07.030, 2014.

Kaiser, K., and Zech, W.: Defects in estimation of aluminum in humus complexes of podzolic soils by pyrophosphate extraction, Soil Sci., 161, 452–458, https://doi.org/10.1097/00010694-199607000-00005, 1996.

Kalks, F., Noren, G., Mueller, C. W., Helfrich, M., Rethemeyer, J., and Don, A.: Geogenic organic carbon in terrestrial sediments and its contribution to total soil carbon, SOIL, 7, 347–362, https://doi.org/10.5194/soil-7-347-2021, 2021.

Keiluweit, M., Bougoure, J. J., Nico, P. S., Pett-Ridge, J., Weber, P. K., and Kleber, M.: Mineral protection of soil carbon counteracted by root exudates, Nat. Clim. Change, 5, 588–595, https://doi.org/10.1038/nclimate2580, 2015.

Kidinda, L. K., Olagoke, F. K., Vogel, C., Kalbitz, K., and Doetterl, S.: Patterns of microbial processes shaped by parent material and soil depth in tropical rainforest soils, SOIL Discuss. [preprint], https://doi.org/10.5194/soil-2020-80, 2020.

Kleber, M., Mikutta, R., Torn, M. S., and Jahn, R.: Poorly crystalline mineral phases protect organic matter in acid subsoil horizons, Eur. J. Soil Sci., 56, 717–725, https://doi.org/10.1111/j.1365-2389.2005.00706.x, 2005.

Kleber, M., Eusterhues, K., Keiluweit, M., Mikutta, C., Mikutta, R., and Nico, P. S.: Mineral-organic associations: formation, properties, and relevance in soil environments, Elsevier, Oxford, UK, 2015.

Knicker, H.: Pyrogenic organic matter in soil: its origin and occurrence, its chemistry and survival in soil environments, Quatern. Int., 243, 251–263, https://doi.org/10.1016/j.quaint.2011.02.037, 2011.

Köchy, M., Hiederer, R., and Freibauer, A.: Global distribution of soil organic carbon – Part 1: Masses and frequency distributions of SOC stocks for the tropics, permafrost regions, wetlands, and the world, SOIL, 1, 351–365, https://doi.org/10.5194/soil-1-351-2015, 2015.

Kögel-Knabner, I., Guggenberger, G., Kleber, M., Kandeler, E., Kalbitz, K., Scheu, S., Eusterhues, K., and Leinweber, P.: Organo-mineral associations in temperate soils: integrating biology, mineralogy, and organic matter chemistry, J. Plant Nutr. Soil Sc., 171, 61–82, https://doi.org/10.1002/jpln.200700048, 2008.

Kramer, M. G. and Chadwick, O. A.: Climate-driven thresholds in reactive mineral retention of soil carbon at the global scale, Nat. Clim. Change, 8, 1104–1108, https://doi.org/10.1038/s41558-018-0341-4, 2018.

Lacrose, D. T.: Discovering knowledge in data. An introduction to data mining, John Wiley & Sons, Hoboken, New Jersey, USA, 222 pp., 2004.

Lehmann, J., Kinyangi, J., and Solomon, D.: Organic matter stabilization in soil microaggregates: implications from spatial heterogeneity of organic carbon contents and carbon forms, Biogeochemistry, 85, 45–57, https://doi.org/10.1007/s10533-007-9105-3, 2007.

Levene, H.: Robust tests for equality of variances, contribution to probability and statistics essays in honor of Harold Hotelling, Stanford University Press, Stanford, USA, 1960.

Liu, J., Chen, J., Chen, G., Guo, J., and Li, Y.: Enzyme stoichiometry indicates the variation of microbial nutrient requirements at different soil depths in subtropical forests, PLoS ONE 15, e0220599, https://doi.org/10.1371/journal.pone.0220599, 2020.

Martinez, P. and Souza, I. F.: Genesis of pseudo-sand structure in Oxisols from Brazil – a review, Geoderma Regional, 22, e00292, https://doi.org/10.1016/j.geodrs.2020.e00292, 2020.

Mehra, O. P. and Jackson, M. L.: Iron oxide removal from soils and clays by a dithionite-citrate system buffered with sodium bicarbonate, Clay. Clay Miner., 7, 317–327, https://doi.org/10.1346/CCMN.1958.0070122, 1958.

Minasny, B., Stockmann, U., Hartemink, A. E., and McBratney A. B.: Measuring and modelling soil depth functions, in: Digital Soil Morphometrics, Process in Soil Science, edited by: Hartemink A. and Minansny B., Springer, Chambridge, UK, https://doi.org/10.1007/978-3-319-28295-4_14, 2016.

Moder, K.: How to keep the type I error rate in ANOVA if variances are heteroscedastic, Austrian Journal of Statistics, 36, 179–188, https://doi.org/10.17713/ajs.v36i3.329, 2007.

Murphy, E. M., Zachara, J. M., Smith, S. C., and Phillips, J. L.: The sorption of humic acids to mineral surfaces and their role in contaminant binding, Sci. Total Environ., 117/118, 413–423, https://doi.org/10.1016/0048-9697(92)90107-4, 1992.

NASA JPL: NASA shuttle radar topography mission global 1 arc second, 2013, distributed by NASA EOSDIS Land Processes DAAC, NASA JPL, https://doi.org/10.5067/MEaSUREs/SRTM/SRTMGL1.003, 2013.

Oades, J. M.: Soil organic matter and structural stability: mechanisms and implications for management, Plant Soil, 76, 319–337, https://doi.org/10.1007/BF02205590, 1984.

Oades, J. M.: The retention of organic matter in soils, Biogeochemistry, 5, 35–70, https://doi.org/10.1007/BF02180317,1988.

Pan, Y., Birdey, R. A., Fang, J., Houghton, R., Kauppi, P. E., Kurz, W. A., Phillips, O. L., Shvidenko, A., Lewis, S. L., Canadell, J. G., Ciais, P., Jackson, R. B., Pacala, S. W., McGuire, A. G., Piao, S., Rautiainen, A., Sitch, S., and Hayes, D.: A large and persistent carbon sink in the world's forests, Science, 333, 988–993, https://doi.org/10.1126/science.1204588, 2011.

Porder, S., Paytan, A., and Vitousek, P. M.: Erosion and landscape development affect plant nutrient status in the Hawaiian Islands, Oecologia, 142, 440–449, https://doi.org/10.1007/s00442-004-1743-8, 2005.

Quesada, C. A., Paz, C., Oblitas Mendoza, E., Phillips, O. L., Saiz, G., and Lloyd, J.: Variations in soil chemical and physical properties explain basin-wide Amazon forest soil carbon concentrations, SOIL, 6, 53–88, https://doi.org/10.5194/soil-6-53-2020, 2020.

R Core Team: A language and environment for statistical computing, R Foundation for Statistical Computing, 2020.

Raich, J. W., Russell, A. E., Kitayama, K., Parton, W. J., and Vitousek, P. M.: Temperature influences carbon accumulation in moist tropical forests, Ecology, 87, 76–87, https://doi.org/10.1890/05-0023, 2006.

Schimel, D., Pavlick, R., Fisher, J. B., Asner, G. P., Saatchi, S., Townsend, P., Miller, C., Frankenberg, C., Hibbard, K., and Cox, P.: Observing terrestrial ecosystems and the carbon cycle from space, Glob. Change Biol., 21, 1762–1776, https://doi.org/10.1111/gcb.12822, 2015.

Schlüter, T. and Trauth, M. H.: Geological atlas of Africa: with notes on stratigraphy, tectonics, economic geology, geohazards and geosites of each country, Springer, Berlin, New York, 272 pp., 2006.

Schmidt, M. W. I., Torn, M. S., Abiven, S., Dittmar, T., Guggenberger, G., Janssens, I. A., Kleber, M., Kögel-Knabner, I., Lehmann, J., Manning, D. A. C., Nannipieri, P., Rasse, D. P., Weiner, S., and Trumbore, S. E.: Persistence of soil organic matter as an ecosystem property, Nature, 478, 49–56, https://doi.org/10.1038/nature10386, 2011.

Schuppli, P. A., Ross, G. J., and McKeague, J. A.: The effective removal of suspended materials from pyrophosphate extracts of soils from tropical and temperate regions, Soil Sci. Soc. Am. J., 47, 1026–1032, https://doi.org/10.2136/sssaj1983.03615995004700050037x, 1983.

Shi, Z., Allison, S. D., He, Y., Levine, P. A., Hoyt, A. M., Beem-Miller, J., Zhu, Q., Wieder, W. R., Trumbore, S. E., and Randerson, J. T.: The age distribution of global soil carbon inferred from radiocarbon measurements, Nat. Geosci., 13, 555–559, https://doi.org/10.1038/s41561-020-0596-z, 2020.

Silver, W. L., Lugo, A. E., and Keller, M.: Soil oxygen availability and biogeochemistry along rainfall and topographic gradients in upland wet tropical forest soils, Biogeochemistry, 44, 301–328, https://doi.org/10.1023/A:1006034126698, 1999.

Simpson, R. T., Frey, S. D., Six, J., and Thiet, R. K.: Preferential accumulation of microbial carbon in aggregate structures of no-tillage soils, Soil Sci. Soc. Am. J., 68, 1249–1255, https://doi.org/10.2136/sssaj2004.1249, 2004.

Six, J., Elliot, E. T., and Paustian, K.: Soil macroaggregate turnover and microaggregate formation: a mechanism for C sequestration under no-tillage agriculture, Soil Biol. Biochem., 32, 2099–2103, https://doi.org/10.1016/S0038-0717(00)00179-6, 2000a.

Six, J., Paustian, K., Elliot, E. T., and Combrink, C.: Soil structure and organic matter: I. distribution of aggregate-size classes and aggregate-associated carbon, Soil Sci. Soc. Am. J., 64, 681–689, 2000b.

Six, J., Feller, C., Denef, K., Ogle, S., de Moraes Sa, J. C., and Albrect, A.: Soil organic matter, biota and aggregation in temperate and tropical soils – effects of no tillage, Agronomie, 22, 755–775, https://doi.org/10.1051/agro:2002043, 2002.

Six, J., Bossuyt, H., Degryze, S., and Denef, K.: A history of research on the link between (micro)aggregates, soil biota, and soil organic matter dynamics, Soil Till. Res., 79, 7–31, https://doi.org/10.1016/j.still.2004.03.008, 2004.

Smith, K.: Metal sorption on mineral surfaces: an overview with examples relating to mineral deposits, Rev. Econ. Geol., 6, 161–198, https://doi.org/10.5382/Rev.06.07, 1999.

Souza, I. F., Almeida, L. F. J., Jesus, G. L., Kleber, M., and Silva, I. R.: The mechanisms of organic carbon protection and dynamics of C-saturation in Oxisols vary with particle-size distribution, Eur. J. Soil Sci., 68, 726–739, https://doi.org/10.1111/ejss.12463, 2017.

Stewart, C. E., Plante, A. F., Paustian, K., Conant, R. T., and Six, J.: Soil carbon saturation: linking concept and measurable carbon pools, Soil Biol. Biochem., 72, 379–392, https://doi.org/10.2136/sssaj2007.0104, 2008.

Stone, M. M., DeForest, J. L., and Plante, A. F.: Changes in extracellular enzyme activity and microbial community structure with soil depth at the Luquillo Critical Zone Observatory, Soil Biol. Biochem., 75, 237–247, https://doi.org/10.1016/j.soilbio.2014.04.017, 2014.

Stucki, J. W., Goodman, B. A., and Schwertmann, U.: Iron in soils and clay minerals, Springer, Dordrecht, Netherlands, 894 pp., 1988.

Stuiver, M. and Polach, A. H.: Discussion reporting of ^{14}C data, Radiocarbon, 19, 355–363, https://doi.org/10.1017/S0033822200003672, 1977.

Tamhane, A. C.: A comparison of procedures for multiple comparisons of means with unequal variances, J. Am. Stat. Assoc., 74, 471–480, https://doi.org/10.2307/2286358, 1979.

Tardy, Y. and Nahon, D.: Geochemistry of laterites, stability of Al-goethite, Al-hematite, and Fe3+-kaolinite in bauxites and ferricretes: an approach to the mechanism of concretion formation, Am. J. Sci., 285, 865–903, 1985.

Trumbore, S.: Age of soil organic matter and soil respiration: radiocarbon constraints on belowground C dynamics, Ecol. Appl., 10, 399–411, https://doi.org/10.1890/1051-0761(2000)010[0399:AOSOMA]2.0.CO;2, 2000.

Trumbore, S.: Radiocarbon and soil carbon dynamics, Annu. Rev. Earth Pl. Sc., 37, 47–66, https://doi.org/10.1146/annurev.earth.36.031207.124300, 2009.

van Breugel, P., Kindt, R., Lillesø, J. P. B., Bingham, M., Demissew, S., Dudley, C., Friis, I., Gachathi, F., Kalema, J., Mbago, F., Moshi, H. N., Mulumba, J., Namaganda, M., Ndangalasi, H. J., Ruffo, C. K., Védaste, M., Jamnadass, R., and Graudal,

L.: Potential natural vegetation map of Eastern Africa (Burundi, Ethiopia, Kenya, Malawi, Rwanda, Tanzania, Uganda and Zambia): Version 2.0, Forest and Landscape (Denmark) and World Agroforestry Centre (ICRAF), Nairobi, Kenia & Copenhagen, Denmark, 2020.

van der Voort, T. S., Mannu, U., Hagedorn, F., McIntyre, C., Walthert, L., Schleppi, P., Haghipour, N., and Eglinton, T. I.: Dynamics of deep soil carbon – insights from ^{14}C time series across a climatic gradient, Biogeosciences, 16, 3233–3246, https://doi.org/10.5194/bg-16-3233-2019, 2019.

Van Hemelryck, H., Fiener, P., Van Oost, K., Govers, G., and Merckx, R.: The effect of soil redistribution on soil organic carbon: an experimental study, Biogeosciences, 7, 3971–3986, https://doi.org/10.5194/bg-7-3971-2010, 2010.

van Keulen, H.: (Tropical) soil organic matter modelling: problems and prospects, Nutr. Cycl. Agroecosys., 2001, 33–39, https://doi.org/10.1023/A:1013372318868, 2001.

von Lützow, M., Kögel-Knabner, I., Ekschmitt, K., Flessa, H., Guggenberger, G., Matzner, E., and Marschner, B.: SOM fractionation methods: relevance to functional pools and to stabilization mechanisms, Soil Biol. Biochem., 39, 2183–2207, https://doi.org/10.1016/j.soilbio.2007.03.007, 2007.

Vereecken, H., Schnepf, A., Hopmans, J. W., Javaux, M., Or, D., Roose, T., Vanderborght, J., Young, M. H., Amelung, W., Aitkenhead, M., Allison, S. D., Assouline, S., Baveye, P., Berli, M., Brüggemann, N., Finke, P., Flury, M., Gaiser, T., Govers, G., Ghezzehei, T., Hallett, P., Hendricks Franssen, H. J., Heppell, J., Horn, R., Huisman, J. A., Jacques, D., Jonard, F., Kollet, S., Lafolie, F., Lamorski, K., Leitner, D., McBratney, A., Minasny, B., Montzka, C., Nowak, W., Pachepsky, Y., Padarian, J., Romano, N., Roth, K., Rothfuss, Y., Rowe, E. C., Schwen, A., Šimůnek, J., Tiktak, A., van Dam, J., van der Zee, S. E. A. T. M., Vogel, H. J., Vrugt, J. A., Wöhling, T., and Young, I. M.: Modeling soil processes: review, key challenges, and new perspectives, Vadose Zone J., 15, 1–57, vzj2015.09.0131, https://doi.org/10.2136/vzj2015.09.0131, 2016.

Verhegghen, A., Mayaux, P., de Wasseige, C., and Defourny, P.: Mapping Congo Basin vegetation types from 300 m and 1 km multi-sensor time series for carbon stocks and forest areas estimation, Biogeosciences, 9, 5061–5079, https://doi.org/10.5194/bg-9-5061-2012, 2012.

Vitousek, P., Chadwick, O., Matson, P., Allison, S., Derry, L., Kettley, L., Luers, A., Mecking, E., Monastra, V., and Porder, S.: Erosion and the rejuvenation of weathering-derived nutrient supply in an old tropical landscape, Ecosystems, 6, 762–772, https://doi.org/10.1007/s10021-003-0199-8, 2003.

Wang, J., Sun, J., Xia, J., He, N., Li, M., and Niu, S.: Soil and vegetation carbon turnover times from tropical to boreal forests, Funct. Ecol., 32, 71–82, https://doi.org/10.1111/1365-2435.12914, 2018.

Wang, Y. P., Law, R. M., and Pak, B.: A global model of carbon, nitrogen and phosphorus cycles for the terrestrial biosphere, Biogeosciences, 7, 2261–2282, https://doi.org/10.5194/bg-7-2261-2010, 2010.

Wattel-Koekkoek, E. J. W., Buurman, P., van der Plicht, J., Wattel, E., and van Breemen, N.: Mean residence time of soil organic matter associated with Kaolinite and Smectite, Eur. J. Soil Sci., 54, 269–278, https://doi.org/10.1046/j.1365-2389.2003.00512.x, 2003.

West, G. and Dumbleton, M. J.: The mineralogy of tropical weathering illustrated by some west Malaysian soils, Q. J. Eng. Geol. Hydroge., 3, 25–40, https://doi.org/10.1144/GSL.QJEG.1970.003.01.02, 1970.

Wilcke, W., Yasin, S., Abramowski, U., Valarezo, C., and Zech, W.: Nutrient storage and turnover in organic layers under tropical montane rain forest in Ecuador, Eur. J. Soil Sci., 53, 15–27, https://doi.org/10.1046/j.1365-2389.2002.00411.x, 2002.

Wilken, F., Sommer, M., Van Oost, K., Bens, O., and Fiener, P.: Process-oriented modelling to identify main drivers of erosion-induced carbon fluxes, SOIL, 3, 83–94, https://doi.org/10.5194/soil-3-83-2017, 2017.

Wood, T. E., Cavaleri, M. A., and Reed, S. C.: Tropical forest carbon balance in a warmer world: a critical review spanning microbial- to ecosystem-scale processes, Biol. Rev., 87, 912–927, https://doi.org/10.1111/j.1469-185X.2012.00232.x, 2012.

Zhang, L., Zeng, G., and Tong, C.: A review on the effects of biogenic elements and biological factors on wetland soil carbon mineralization, Acta Ecologica Sinica, 31, 5387–5395, 2011.

Zotarelli, L., Alves, B. J. R., Urquiaga, S., Torres, E., dos Santos, H. P., Paustian, K., Boddey, R. M., and Six, J.: Impact of tillage and crop rotation on aggregate-associated carbon in two Oxisols, Soil Sci. Soc. Am. J., 69, 482–491, 2005.